



Marianne Kräuter, BSc

Deposition of Ion Conductive Membranes from Ionic Liquids by Initiated Chemical Vapour Deposition

MASTER'S THESIS

to achieve the university degree of
Master of Science

Master's Degree Program: Advanced Materials Science

Submitted to

Graz University of Technology

Supervisor

Ass.Prof. Dr. Anna Maria Coclite

Institute of Solid State Physics

Graz, March 2018

AFFIDAVIT

I declare that I have authored this thesis independently, that I have not used other than the declared sources/resources, and that I have explicitly indicated all material which has been quoted either literally or by content from the sources used. The text document uploaded to TUGRAZonline is identical to the present master's thesis.

Date

Signature

ABSTRACT

Ionic Liquids are salts which are liquid at room temperature. Their excellent ion conductivity makes them highly attractive for a large variety of applications, amongst others electrochemical applications such as fuel cells or various organic electronic devices. For many applications, however, it would be much easier to handle ionic liquids in a solid state, in form of a membrane.

Initiated chemical vapour deposition (iCVD) is an experimental technique which allows uniform thin-film coatings with controlled material composition. ICVD holds many advantages over other thin film techniques: the substrate can be held near room temperature and the thickness of the growing film can be controlled in-situ during the process. Additionally, there no decomposition of materials occurs and the whole process is solvent-free.

This thesis comprises the experimental realisation of solidified ionic liquid films via iCVD and optimisation of experimental parameters. The films are analysed by spectroscopic ellipsometry, fourier transform infra-red spectroscopy, profilometry, electrochemical impedance spectroscopy and dynamic contact angle measurements to investigate their uniformity, topography, chemical state as well as their conductivity.

The results show that the obtained films are partly polymerised and sufficiently conductive to use them for the desired applications. It is shown how various experimental parameters influence the homogeneity, degree of polymerisation and conductivity of the resulting membranes.

KURZFASSUNG

Ionische Flüssigkeiten sind Salze, die bei Raumtemperatur flüssig sind. Aufgrund ihrer exzellenten Ionenleitfähigkeit sind sie für eine Vielzahl von Anwendungsgebieten höchst attraktiv, darunter elektrochemische Anwendungen, wie Brennstoffzellen oder unterschiedliche organische elektronische Bauteile. Für viele Anwendungen wäre es jedoch viel einfacher Ionische Flüssigkeiten in einem festen Aggregatzustand, in Form einer Membran, handzuhaben.

Initiierte chemische Gasphasenabscheidung (iCVD) ist eine experimentelle Technik, die es erlaubt, gleichförmige Dünnschichten mit kontrollierter Materialzusammensetzung abzuscheiden. Im Vergleich mit anderen Dünnschichttechniken, weist iCVD viele Vorteile auf: Das Substrat kann nahe der Raumtemperatur temperiert werden und die Dicke der abgeschiedenen Schicht kann in situ während des Prozesses gemessen werden. Darüber hinaus findet keine Zersetzung der verwendeten Materialien statt und die Technik ist vollkommen lösungsmittelfrei.

Diese Arbeit beinhaltet die experimentelle Realisierung polymerisierter Filme aus ionischer Flüssigkeit und die Optimierung der Versuchsparameter. Die Filme werden mit spektroskopischer Ellipsometrie, Fourier-Transformations-Infrarotspektroskopie, Profilometrie, elektrochemischer Impedanz-Spektroskopie sowie dynamischen Kontaktwinkelmessungen analysiert, um deren Oberflächenbeschaffenheit, chemischen Zustand und spezifische Leitfähigkeit zu untersuchen.

Die Ergebnisse zeigen, dass die resultierenden Filme teilweise polymerisiert und ausreichend leitfähig sind, um sie für die gewünschten Anwendungen zu verwenden. Es wird gezeigt, welchen Einfluss experimentelle Parameter auf Homogenität, Grad der Polymerisation und Leitfähigkeit der resultierenden Membranen haben.

ACKNOWLEDGMENTS

Above all I would like to thank my supervisor Ass.Prof. Dr. Anna Maria Coclite for her supportive and motivating guidance throughout the thesis.

Furthermore, I am grateful for the time I spend with my wonderful colleagues; it was a pleasure sharing an office with you! I especially want to thank Alberto Perrotta for showing me the ropes concerning impedance spectroscopy, Martin Tazreiter for sharing his superior knowledge in all things with me during the first few months of work and Paul Christian for taking over in that regard after Martin had left. I also thank Katrin Unger for making the working environment in the office more comfortable and cheerful than I could have ever imagined.

I am also thankful to all helpers outside our group, mainly Harald Kerschbaumer, Birgit Kunert, and Elisabeth Stern, who keep the institute running. Thank you also to Prof. Gregor Trimmel from the Institute for Chemistry and Technology of Materials of the Graz University of Technology for letting me use the profilometer of his group for my experiments.

Last but not least, I want to say that I am immensely thankful to my parents and family for their lifelong support and love in everything I do. Thank you for believing in me!

CONTENTS

1	INTRODUCTION	1
I	FUNDAMENTALS	3
2	POLYMERS	5
2.1	Co-polymers	5
2.2	Radical Chain Polymerisation	5
2.3	Proton Conduction Mechanisms	7
3	IONIC LIQUIDS	9
4	INITIATED CHEMICAL VAPOUR DEPOSITION	11
4.1	Deposition Process	11
4.2	Important Parameters	12
4.3	Advantages	12
4.4	Polymerisation of Ionic Liquid	13
5	ELECTROCHEMICAL IMPEDANCE SPECTROSCOPY	15
5.1	Resistance vs. Impedance	15
5.2	Resistance Measurements	16
5.3	Electrochemical Impedance Spectroscopy Measurements	17
5.4	Conductivity	19
II	EXPERIMENTAL	23
6	EXPERIMENTAL SET-UP AND USED CHEMICALS	25
6.1	iCVD Set-up	25
6.2	Used Chemicals	26
7	SAMPLE PREPARATION	29
7.1	Substrates and Their Pre-treatment	29
7.2	Transferring Ionic Liquid onto the Substrate	30
7.3	Polymerising Ionic Liquid via Initiated Chemical Vapour Deposition	33
8	CHARACTERISATION TECHNIQUES	37
8.1	Spectroscopic Ellipsometry	37
8.2	Dynamic Contact Angle Measurements (dCAM)	38
8.3	Profilometry	39
8.4	Fourier Transform Infrared Spectroscopy (FTIR)	40
8.5	Electrochemical Impedance Spectroscopy (EIS)	40
III	RESULTS AND DISCUSSION	43
9	TUNING DEPOSITION PARAMETERS	45
9.1	Stable Polymer Films	45
9.2	Effect of Pre-coating on Uniformity of Layers	45
9.2.1	Dynamic Contact Angle Measurements	46
9.2.2	Profilometry	46
9.3	Investigating the Degree of Polymerisation	48

10	RESISTIVITY AND CONDUCTIVITY	55
10.1	Fitting Models for Resistivity Results	55
10.2	Conductivity Results	58
10.2.1	Comparison to Literature Values	62
10.2.2	Comparison to Previous Studies	63
10.3	Ageing of Samples	64
11	CONCLUSION AND OUTLOOK	67
	BIBLIOGRAPHY	69

LIST OF FIGURES

Figure 1	Types of co-polymers	6
Figure 2	EGDMA-HEMA-network	6
Figure 3	Proton transport mechanisms	8
Figure 4	Cations and anions used in ionic liquids	9
Figure 5	Fields of application for ionic liquids	10
Figure 6	iCVD set-up	11
Figure 7	iCVD process	12
Figure 8	Two-point vs. four-point measurements	17
Figure 9	Equivalent circuit for two-point measurements	19
Figure 10	Commonly encountered impedance responses	20
Figure 11	Cuboid	21
Figure 12	iCVD reactor	25
Figure 13	In-situ thickness control during iCVD	27
Figure 14	Used chemicals	28
Figure 15	Produced sample types	29
Figure 16	Printed Circuit Board	30
Figure 17	Ellipsometer device	37
Figure 18	Principle of contact angle measurements	39
Figure 19	Profilometer device	40
Figure 20	EIS measurement device	41
Figure 21	Determining composition of stable polymer film	46
Figure 22	Results from dynamic contact angle measurements	47
Figure 23	Results of profilometry measurements	47
Figure 24	FTIR spectrum of solidified IL	49
Figure 25	Free-standing IL membrane	50
Figure 26	Effect of deposition parameters on polymerisation (Pt.1)	51
Figure 27	Effect of deposition parameters on polymerisation (Pt.2)	52
Figure 28	Partly solidified IL film	52
Figure 29	Undesired effects when transferring IL onto substrate	53
Figure 30	Fitting models to describe obtained EIS data .	55
Figure 31	Fitting models employed on EIS measurements	56
Figure 32	Resistance measurement results	57
Figure 33	Conductivity results	59
Figure 34	Ionic Liquid: EMID	62
Figure 35	Conductivity of p-(MAA-HEMA-EGDMA) . .	63
Figure 36	Ageing of samples	65

LIST OF TABLES

Table 1	Variables used in figures and formulas	15
Table 2	Circuit elements used for fitting equivalent circuits	18
Table 3	Pre-coating depositions via iCVD	31
Table 4	Transfer of IL onto substrates	32
Table 4	Continued: Transfer of ionic liquid onto substrates	33
Table 5	iCVD coatings to solidify IL	34
Table 5	Continued: Coatings performed to solidify IL	35
Table 6	Conductivity Values	60
Table 6	Continued: Resistivity and conductivity values of measured samples	61
Table 6	Continued: Resistivity and conductivity values of measured samples	62

ACRONYMS

AC	alternating current
AMID	1-Allyl-3-methylimidazolium dicyanamide
CPE	constant phase element
DC	direct current
dCAM	dynamic contact angle measurement
EGDMA	ethylene glycol dimethacrylate
EIS	electrochemical impedance spectroscopy
EMID	1-ethyl-3-methylimidazolium dicyanamide
FTIR	fourier transform infrared spectroscopy
HEMA	2-Hydroxyethyl methacrylate
iCVD	initiated chemical vapour deposition
IL	ionic liquid
MAA	methacrylic acid

INTRODUCTION

Ionic liquids are liquid salts that exhibit high proton or anion conductivities, making them highly attractive for a large variety of new applications, including their use as ion conductive membranes for organic micro-electronic devices [1] or utilising them as proton exchange membranes in fuel cells [2]. Fuel cells convert chemical energy from a fuel into electricity through an electrochemical reaction and provide a very clean, cheap and highly efficient production of electrical energy, thus becoming increasingly important for the automobile industry and power generation, especially in remote locations such as spacecraft or rural areas. However, commonly used materials for ion conductive membranes, such as Nafion, are very expensive, calling for an alternative production approach [3].

This master's thesis focuses on developing a way to solidify ionic liquids in order to produce ion conductive membranes, that retain a sufficiently high conductivity to apply them in various fields.

The solidification process is performed via initiated Chemical Vapor Deposition (iCVD). Invented at MIT, iCVD is a novel method to synthesize conformal thin films and shows big advantages over other conventional thin film deposition techniques, since it works solvent free at relatively low temperatures, which allows to coat a vast variety of substrates. Monomers, cross-linkers and the so called initiator molecules are introduced to the reactor chamber, where hot filaments (200-300 °C) break the initiator molecules to radicals, which react then with the monomers adsorbed on the cooled substrate surface [4].

To obtain homogenous and stable membranes various experimental parameters are tuned. The resulting samples are characterized with various methods (including electrochemical impedance spectroscopy (EIS), infrared spectroscopy (FTIR) and Ellipsometry) to investigate their topological, optical and electrical properties.

The first part of this thesis provides the fundamentals of polymers and ionic liquids as well as initiated chemical vapour deposition and explain the physical principle behind electrochemical impedance spectroscopy.

In the second part, the experimental set-up, the procedure of sample preparation and the characterisation techniques used to gain insight into the properties of the obtained IL films are introduced.

The third part covers the results obtained with the characterisation techniques detailed in part 2 and discusses them.

Part I

FUNDAMENTALS

This part is concerned with the description of important fundamentals for the work conducted for this thesis. After delving into the theory of polymers and ionic liquids, the process of initiated chemical vapour deposition as well as the theory behind electrochemical impedance spectroscopy is discussed.

POLYMERS

A polymer is a macromolecule built up of many, rather simple molecules to a long, chain-like structure by a process called polymerisation. The simple compounds whose molecules form the polymers are called monomers. They are connected to each other by covalent bonds and provide a backbone, to which other atoms or molecules can attach. In comparison to smaller molecules, polymer networks exhibit very distinct physical properties. The high molecular weight and the strong intermolecular bonds lead to higher melting points or special properties like viscoelasticity [5].

2.1 CO-POLYMERS

A polymer is termed a homo-polymer, if it consists of only one monomer species. If it consists of more than one type of monomer, it is categorised as a co-polymer. Co-polymers consisting of two monomer species A and B can be classified according to the order in which the repeating units are linked together (also shown in fig. 1)

- *Alternating co-polymers*: ...-A-B-A-B-A-B-...
- *Statistic co-polymers* exhibit a randomly generated sequence: e.g.: ...-B-A-B-B-B-A-B-A-A-B-...
- *Block copolymers* have smaller homo-polymer chains covalently bonded together to a bigger chain: ...-A-A-A-B-B-B-...
- *Graft co-polymers* are characterised by side chains of one species being bound to the main chain of the other species [5].

Mechanical properties of polymers can be further enhanced by adding a cross-linker. This monomer connects the linear polymer chains, forming a cross-linked polymer network, as shown in the example in fig. 2. The cross-linker drastically increases the stability of polymer thin films [6].

2.2 RADICAL CHAIN POLYMERISATION

One way of forming a polymer from monomers is called *radical chain polymerisation*. For this polymerisation technique unsaturated monomer molecules add onto the active site of a growing polymer chain. Growth of the polymer occurs only at ends of the chain and proceeds exclusively by reactions between monomers and active sites

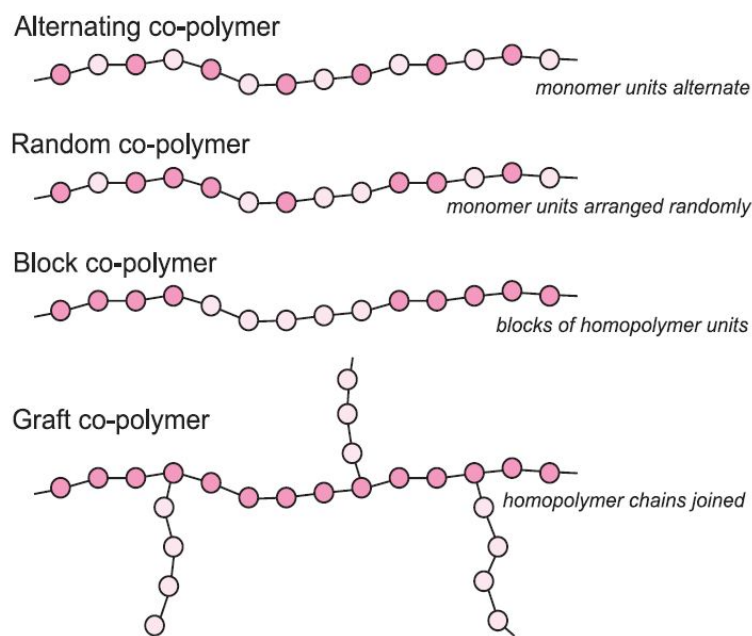


Figure 1: Different types of co-polymers consisting of two monomers. Image reprinted from [5].

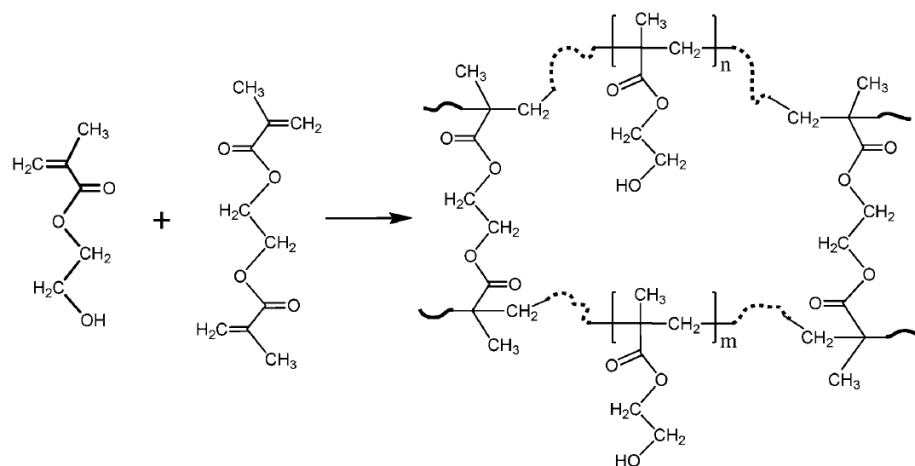


Figure 2: Example to illustrate the stabilising effect of a cross-linker on a polymer: EGDMA employed as a cross-linker in a HEMA network. Image reprinted from [6].

on the polymer chain with regeneration of the active sites at the end of each growth step.

Usually, chain-growth polymerisation consists of the following steps:

1. *Chain Initiation*: Commonly, an initiator generates active centres and thus starts the chemical process. Typical initiators include organic compounds with a labile group like peroxide (-O-O-).
2. *Chain Propagation*: An active centre on the growing polymer molecule adds one monomer molecule so that a new polymer molecule is formed, which is one repeat unit longer with a new active centre.
3. *Chain Termination*: Termination happens when free radicals combine and thus end the polymerisation process [7].

In contrast to step-growth mechanism, which uses the functional groups of the monomer, chain growth polymerisation utilises the free-radical or ion groups. A high-molecular-weight polymer is formed immediately in a chain polymerisation, since a radical adds many monomer units in a chain reaction and grows rapidly to a large size. Whereas in chain polymerisation only monomer and the propagating species can react with each other, any two molecular species present can react in step polymerisation. Long reaction times are necessary in step polymerisation for both high percent conversion and high molecular weights [8].

2.3 PROTON CONDUCTION MECHANISMS

Polymers which partly consist of units with ionic or ionisable groups are called ionomers [9]. Those groups are responsible for the ion-conductivity of the ionomers. For various applications such as polymer electrolyte membranes (PEMs) [10] or organic electrochemical devices [1] proton conduction is of particular interest. The transport of protons in ionomers can be described by three mechanisms, which are further illustrated in fig. 3:

- *Proton hopping or Grotthuss mechanism*: Proton hopping describes the transport of an excess proton in water by hopping from one water molecule to the next.
- *Vehicular mechanism*: A proton forms a complex together with water molecules and drifts through the medium. This type of transport describes the diffusive transport of the proton-solvent molecule complex (e.g. the hydronium ion). This mechanism is typically characterised by lower proton mobility since strong hydrogen bonding is absent.

- *Direct transportation*: If the mobile ends of polymer chains carry a negative charge they can pass a positively charged ion on to a neighbouring chain. This requires the polymer to be in an unordered state.

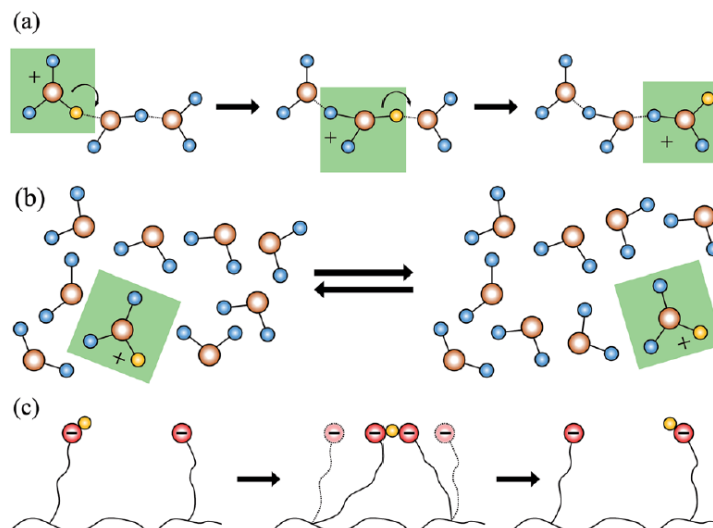


Figure 3: Proton transport mechanisms, reprinted from [11].

- a... Proton hopping
- b... vehicle mechanism
- c... direct transportation

The number of available charge carriers, depending on the solvation state of the acid groups, directly influences the conductivity [12].

IONIC LIQUIDS

Ionic liquids are organic salts with a melting point below 100 °C, often even below room temperature. Their low melting point is caused by a disturbance of the long range order of the crystal lattice. Steric hindrance or charge de-localisation causes a reduction of the lattice energy.

Ionic liquids are composed of an organic cation and an organic or inorganic anion [13]. A few examples for possible cations and anions can be seen in fig. 4.

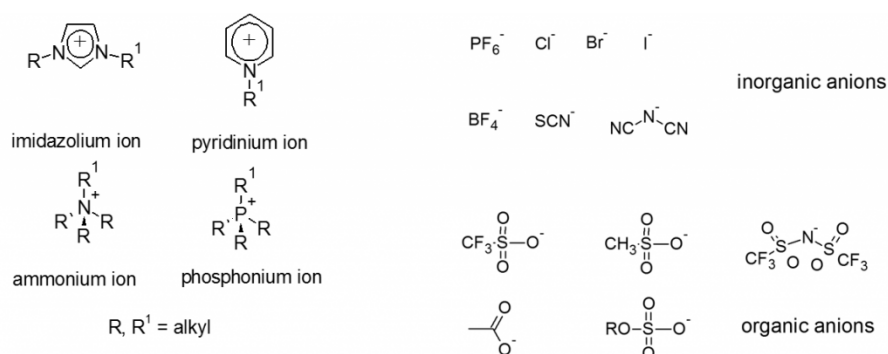


Figure 4: Examples of cations and anions used in ionic liquids. Figure reprinted from [13].

The ability to mix and match the cationic and anionic constituents of ionic liquids and to functionalise their side chains makes tuning its properties possible. Tunable properties include conductivity, viscosity, solubility of diverse solutes as well as miscibility with a wide range of solvents. Additionally, their minimal vapour pressure, their high ionic conductivity and their relative insensitivity to air and water make them highly attractive for a broad field of applications including but not limited to electro-elastic materials, heat storage purposes, separation techniques, employing them as electrolytes or liquid crystals [14]. Fig. 5 gives an overview of possible fields of application for ionic liquids.

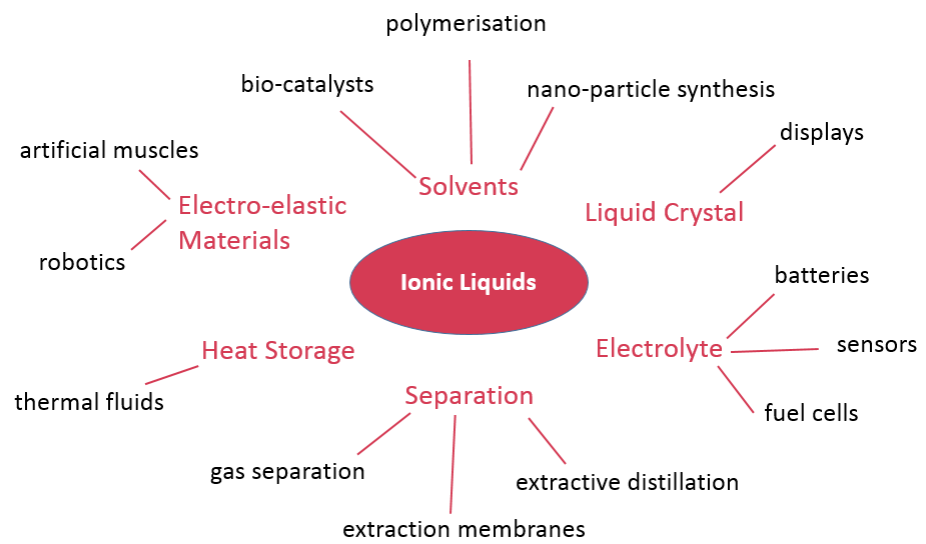


Figure 5: An Overview of possible fields of application for ionic liquids

INITIATED CHEMICAL VAPOUR DEPOSITION

Initiated chemical vapour deposition (iCVD) is a rather novel thin film deposition method which involves many components expected of any CVD process such as precursor selection, vapour delivery, a reaction chamber, temperature and pressure control, exhaust management, a vacuum pump system and process monitoring. However, iCVD differs in several important features from conventional CVD [4]. Fig. 6 illustrates a typical iCVD set-up.

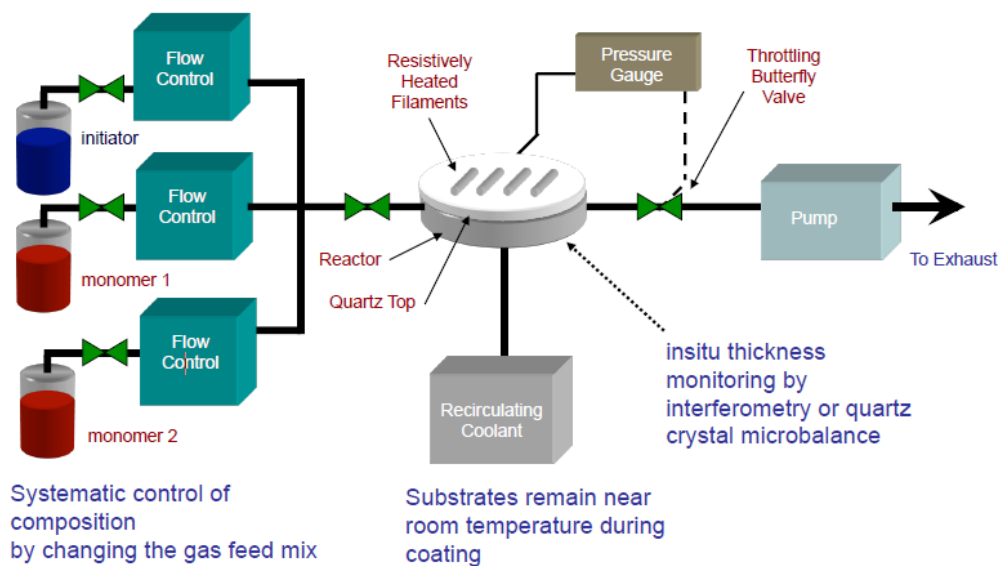


Figure 6: Typical set-up for initiated chemical vapour deposition

4.1 DEPOSITION PROCESS

The iCVD process involves the following main steps:

- Firstly, the thermal decomposition of an initiator in vapour phase takes place to form primary radicals. This happens at the top of the reactor at a filament heated to 200 °C – 400 °C.
- Secondly, the primary radicals as well as the heated monomers diffuse to a surface in vapour phase and adsorb there. The substrate is kept at a much lower temperature than the filaments, typically below 50 °C to promote adsorption of the materials.
- Thirdly, the actual polymerisation, which follows the same steps as conventional free-radical polymerisation (as described

in sec.2.2), takes place via initiation, propagation and termination events.

Thus polymerisation of the monomers on the surface occurs and a continuous polymer coating is formed. During this process the initiator radicals only react with the vinyl bonds of a monomer, leaving the other groups unharmed [15]. Fig.7 illustrates this process. The polymerisation process [16] as well as a corresponding kinetic model [17] have been explained in detail in literature.

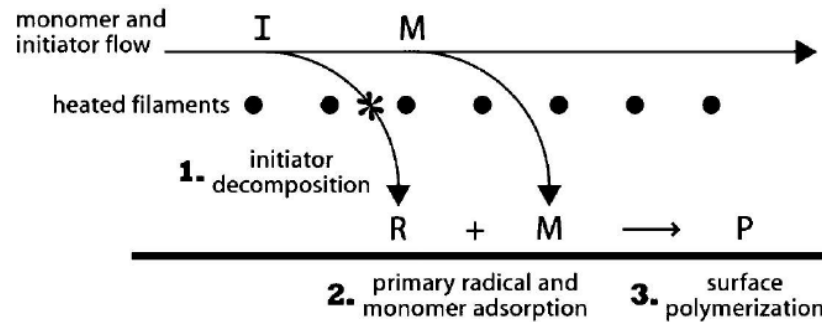


Figure 7: Illustration of the iCVD-process as described in sec. 4.1. Figure reprinted from [4].

4.2 IMPORTANT PARAMETERS

Monomer flow rate as well as temperature of substrate and filament influence the deposition kinetics. Low substrate temperatures, for instance, enhance the absorption of monomer units and thus increase the deposition rate. However, it is the ratio between the monomer partial pressure (P_m) and the saturation pressure at the substrate temperature (p_{sat}) that is the dominant parameter. $\frac{P_m}{p_{sat}}$ is defined as the saturation ratio, S . If this ratio approaches one, a liquid will be in equilibrium with the monomer vapour. Since this is undesirable in the iCVD process, a ratio below one is typically used, which decreases the deposition rate of the film but results in more homogeneous and higher molecular weight films. S determines the concentration of monomer absorbed on the surface, the film growth rate, the number-average molecular weight of the polymer film formed and the degree of con-formality achieved [4].

4.3 ADVANTAGES

In contrast to common techniques such as spraying, dipping or spin coating iCVD is completely solvent-free. This allows to coat substrates which would be dissolved by a solvent and also avoids problems that could arise due to different solubilities of the used

monomers in a solvent. Furthermore, the lack of any solvent avoids thickness variations due to surface tension effects and the surface diffusion of the absorbed species prior to polymerisation leads to very conformal coatings [18]. Since the substrate is held at low temperatures (typically near room temperature [16]) iCVD allows to coat a large variety of substrates including ones that would not survive high temperatures employed in other methods such as plasma assisted techniques. Another big advantage of iCVD is the production of stoichiometric polymers which resemble addition polymers from solution, just without using a solvent [18].

4.4 PROPOSED IDEAL POLYMERISATION MECHANISM OF IONIC LIQUID BY INITIATED CHEMICAL VAPOUR DEPOSITION

For the polymerisation process proposed in the following, ionic liquids with vinyl bonds have to be chosen. The ideal polymerisation process for ionic liquids via iCVD is proposed as follows:

Initiator radicals activate the vinyl bonds at the surface and near the surface of the ionic liquid. When the monomer is flown into the reaction chamber it not only polymerises the bonds directly at the surface of the ionic liquid but also partly diffuses into the liquid, if the molecular size of the employed monomer is chosen correctly. A cross-linker stabilises the resulting film, as shown in sec. 2.1. Thus the ionic liquid will be partly polymerised, almost encapsulated by a polymer layer. That such an encapsulation is possible without polymerising the ionic liquid inside has been shown in previous studies [19]. It is thought that this will help to retain high mobility of the mobile conducting ions.

THEORY OF ELECTROCHEMICAL IMPEDANCE SPECTROSCOPY

This chapter will start with a short explanation of the concept of impedance before detailing how it can be measured with electrochemical impedance spectroscopy and how the conductivity of samples can be obtained from those measurements. Tab. 1 lists all variables introduced in this section.

Table 1: Variables used in figures and formulas

name	symbol	unit
capacitance	C	F
voltage	U	V
current	I	A
impedance	Z	Ω
inductance	L	H
angular frequency	ω	radian
admittance	Q_0	$\frac{s^n}{\Omega}$
Warburg coefficient	A_w	$\frac{\Omega}{\sqrt{s}}$
current density	\vec{j}	$\frac{A}{m^2}$
electric field	\vec{E}	$\frac{V}{m}$
conductivity	σ	$\frac{1}{\Omega m}$
resistivity	ρ	Ωm
width	a	m
thickness	b	m
length	l	m
area	A	m^2
resistance	R	Ω
charge carrier density	n	$\frac{As}{m^3}$
elementary charge	e	As
mobility	μ	$\frac{m^2}{Vs}$

5.1 RESISTANCE VS. IMPEDANCE

Resistance is the ability of a circuit element to resist the flow of electrical current. A variable which is defined by the well-known Ohm's law, $R = \frac{U}{I}$, with U denoting the electrical voltage and I standing

for the electrical current. But this relationship is limited to only one circuit element, the ideal resistor. The ideal resistor exhibits many limiting qualities:

- It follows Ohm's Law at all current and voltage levels
- Its resistance value is independent of frequency.
- AC current and voltage signals through a resistor are in phase with each other.

Many circuit elements show a far more complex behaviour and thus force us to abandon the simple concept of resistance. In its place we use the more general *impedance*. Impedance is also a measure of the ability of a circuit to resist the flow of electrical current, but unlike resistance it is not limited by the simplifying properties listed above [20].

5.2 RESISTANCE MEASUREMENTS: TWO-POINT VS. FOUR-POINT SET-UPS

Resistance is commonly measured in one of two set-ups: The two-point or the four-point set-up. The most simple resistance measurement set-up is the two point direct current (DC) measurement set-up (see fig. 8). If the object which is to be measured is a usual electron-conductive ohmic resistor, the contact impedances, Z_c , can often be modelled as ohmic resistors. If this contact resistance is much less than the resistance of the object, the latter can be approximated by dividing the applied voltage through the measured current. But, if the object is an electrolyte instead, the circumstances are more complicated. The current is not carried by electrons through all mediums any more, but by ions in the electrolyte. If the current passes through the interface between electrodes and electrolyte, electrochemical reactions occur at the interfaces, which act as sources and sinks for the electrons and ions. Since, in this case, the contact impedances exhibit non-linear current voltage characteristics (often described by the Butler Volmer Equation [21]) two-point DC measurements are not suitable to determine the bulk resistance. Instead a two-point alternating current (AC) measurement is performed at different frequencies to be able to distinguish the contact impedance from the bulk impedance and at small voltages to avoid non-linear behaviour. This measurement is called *two-point impedance spectroscopy*.

A different method to determine the bulk resistance are four-point resistance measurements (as shown in fig. 8). Its main advantage over the two-point set-up being that the influence of the interfaces can be almost eliminated by using it. This results in linear behaviour of the current versus the measured voltage from which the bulk resistance can be concluded by using Ohm's Law. Although this method can be

used for both DC and AC, the AC impedance spectroscopy still has the advantage of avoiding electro-chemical reactions by using small voltages [22].

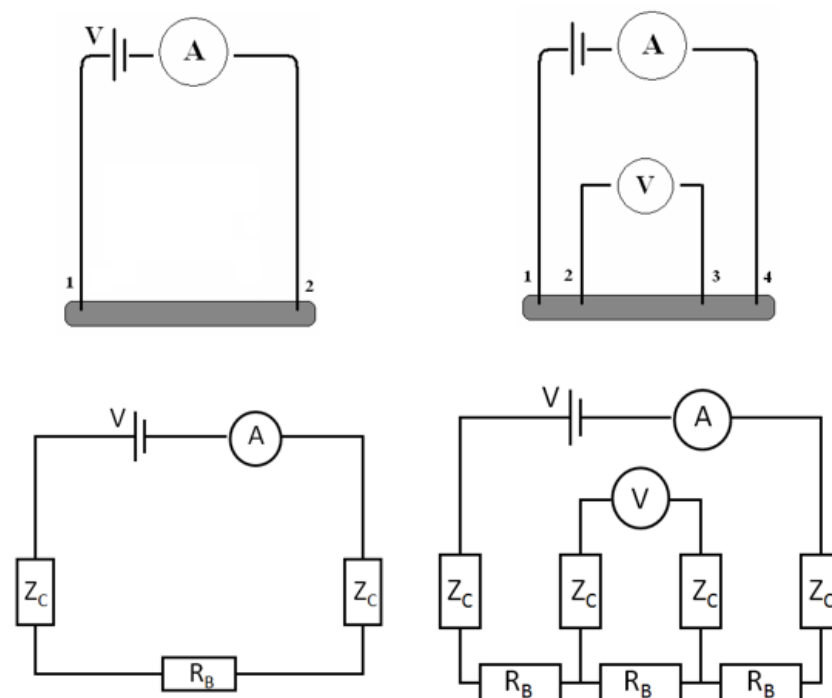


Figure 8: Comparing a two-point impedance spectroscopy measurement set-up (top left) and a four-point set-up (top right). The grey bar represents the measured electrolyte. The two pictures on the bottom show the equivalent circuits for each measurement set-up. Figure reprinted from [22].


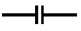



As can be seen from fig. 8, the modelling of an equivalent circuit is considerably easier for two-point measurements than for four-point measurements. It has been shown in literature that two-point measurements are quite accurate for low humidity levels while yielding unreliable results for high humidity measurements [23].

5.3 ELECTROCHEMICAL IMPEDANCE SPECTROSCOPY MEASUREMENTS

Electrochemical impedance spectroscopy is a powerful tool for the characterisation of electrochemical properties of materials used in applications such as fuel cells [23], corrosion protection [24] or batteries [25]. For the measurement a periodic electrical signal is applied to the measurement system and its response is recorded at different frequencies. If the voltage is kept constant, while the current amplitude changes (recommended for high-impedance systems [26]), the measurement is called potentiostatic.

When a two-point AC measurement of an electrolyte is performed, the obtained data should be fitted with the the frequency dependant impedance of the equivalent circuit (shown in fig. 8). But, additionally, the capacity between the electrodes, which is not spotted in a DC measurement, has to be taken into account. Tab. 2 shows standard circuit elements which are used to specify the contact impedance.

Table 2: Circuit elements used for fitting equivalent circuits

R...	resistance		
C...	capacitance		
L...	inductance		
Q_0 ...	admittance ($1/ z $) at $\omega = 1 \text{ rad} \times \text{s}^{-1}$		
ω ...	angular frequency		
A_w ...	Warburg coefficient		
name	impedance	phase ϕ [radians]	symbol
resistor	R	0	
capacitor	$\frac{1}{i\omega C}$	$-\frac{\pi}{2}$	
inductor	$i\omega C$	$\frac{\pi}{2}$	
constant phase element	$\frac{1}{Q_0 \omega^n} e^{-\frac{\pi}{2}nj}$	ϕ	
Warburg impedance	$\frac{A_w}{\sqrt{\omega}} + \frac{A_w}{j\sqrt{\omega}}$	$\frac{\pi}{4}$	

The impedance of the whole circuit can be calculated by iteratively applying the circuit rules for the impedance, Z , of a circuit which consists of two impedances, Z_1 and Z_2 :

Parallel circuit:

$$Z = Z_1 \parallel Z_2 = \frac{1}{\frac{1}{Z_1} + \frac{1}{Z_2}} \quad (1)$$

Serial circuit:

$$Z = Z_1 + Z_2 \quad (2)$$

The constant phase element (CPE) shown in tab. 2. is a generalisation of the first three shown components (resistor, capacitor and inductor), which exhibit special values of the phase, ϕ . CPEs can be used to model the contact impedance, which leads to a two-point equivalent circuit as shown in fig. 9.

The upper part of the equivalent circuit in fig. 9 shows a capacitor which expresses the capacity of the two measurement electrodes. The process of ions moving through the electrolyte and accumulating at the interfaces between electrodes and electrolyte is happening in parallel. Since mirror symmetry is assumed, each interface is modelled with the same CPE. The drift of ions is taken into account with an ohmic resistor. In the ideal case, the contact impedance is a capacitor

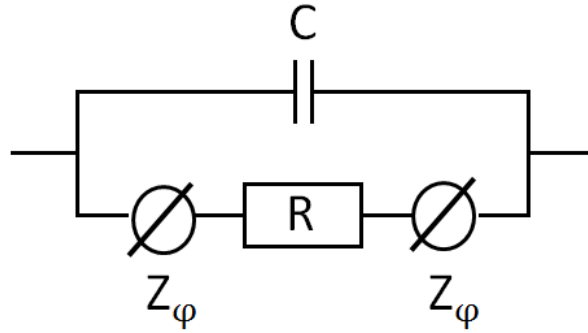


Figure 9: Two-point equivalent circuit for electrolyte measurements. Figure reprinted from [22].

but for real experimental purposes it is advised to use a CPE. Utilising the parallel and serial circuit rules established in eq. 1 and eq. 2 as well as tab. 2 the impedance of this circuit can be calculated as shown in eq. 3.

$$Z = \frac{1}{\frac{1}{R + 2(i\omega)^{\frac{2}{\pi}} \phi^P} + i\omega C} \quad (3)$$

If electrochemical reactions would occur at the interfaces, an additional charge transfer resistance parallel to the CPE would be necessary [22].

Impedance Z can be divided into a real (Z_r) and a complex (Z_j) component, which leads to two common types of graphical representation for impedance data: the *Nyquist* and the *Bode Plot*. The Nyquist plot is a representation of $-Z_j$ as a function of Z_r , while the Bode Plot represents both quantities as a function of frequency. The interpretation of impedance spectroscopy data relies then on modelling the experimental response by an equivalent circuit. However, not every equivalent circuit that matches the experimental data is applicable. Caution has to be taken that the model is also an adequate physical description of the experimental system at hand [20].

Additionally to the detailed example given above in fig. 9, fig. 10 shows commonly encountered impedance responses in their Nyquist representation along with the corresponding equivalent circuits.

5.4 CONDUCTIVITY [22]

Conductivity, σ , is a measure of the ability of a material to conduct electricity. This microscopic local material property is used in the

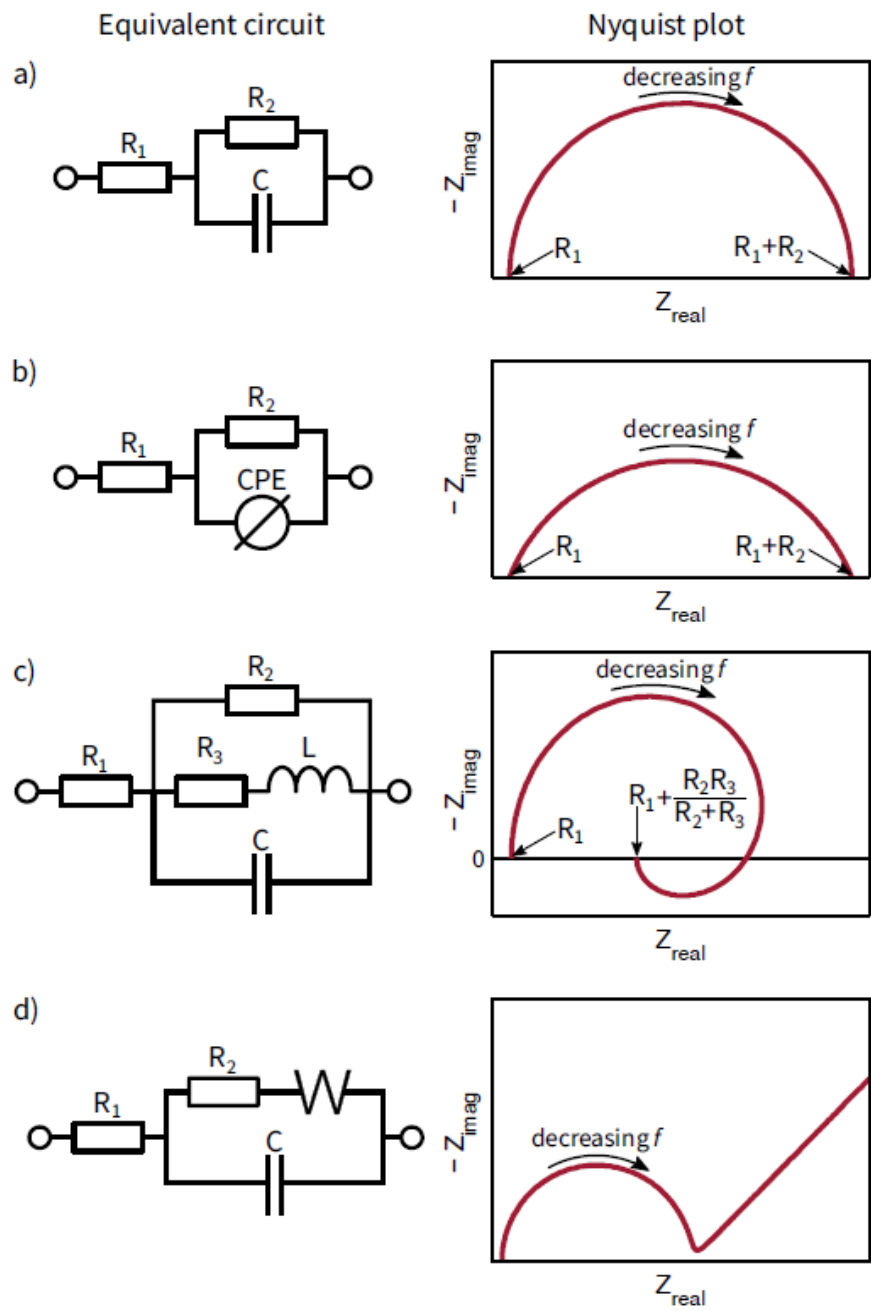


Figure 10: Commonly encountered impedance responses in their Nyquist representation (right) along with the corresponding equivalent circuits (left). Elements that occur in the figure have been introduced in tab. 2. Figure reprinted from [27].

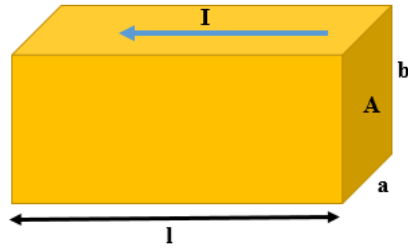


Figure 11: A simple cuboid to illustrate calculations of conductivity as detailed in sec. 5.4.

microscopic Ohms law, $\vec{j} = \sigma \vec{E}$, with the current density \vec{j} and the electric field \vec{E} .

In general, this is a rank two tensor which depends on position. For simplicity we can assume an isotropic medium with a constant conductivity inside it and a conductivity value of zero on the outside. Additionally, if the geometry of the medium is a simple cuboid (as shown in fig. 11) and the electric field is a constant vector pointing along the length l inside the medium, the total current through the area $A = ab$ is given by

$$I = |\vec{j}|A \quad (4)$$

Thus we can calculate the conductivity through

$$\sigma = \frac{1}{\rho} = \frac{1}{AR} = ne\mu \quad (5)$$

The variables used in this chapter are detailed in tab. 1.

Part II

EXPERIMENTAL

This part details the experimental set-up and used chemicals as well as how the examined samples were prepared. The last section of this part contains relevant information on the used characterisation methods.

EXPERIMENTAL SET-UP AND USED CHEMICALS

This chapter details the experimental set-up used for preparing the samples and lists which materials were used in the process.

6.1 ICVD SET-UP

Initiated chemical vapour deposition (iCVD) as described in chapter 4 was used to deposit polymers onto various substrates and to polymerise droplets of ionic liquid (IL) as described in sec. 4.4.

The custom built experimental set-up, which closely follows the schematic picture in fig. 6, is shown in fig. 12.

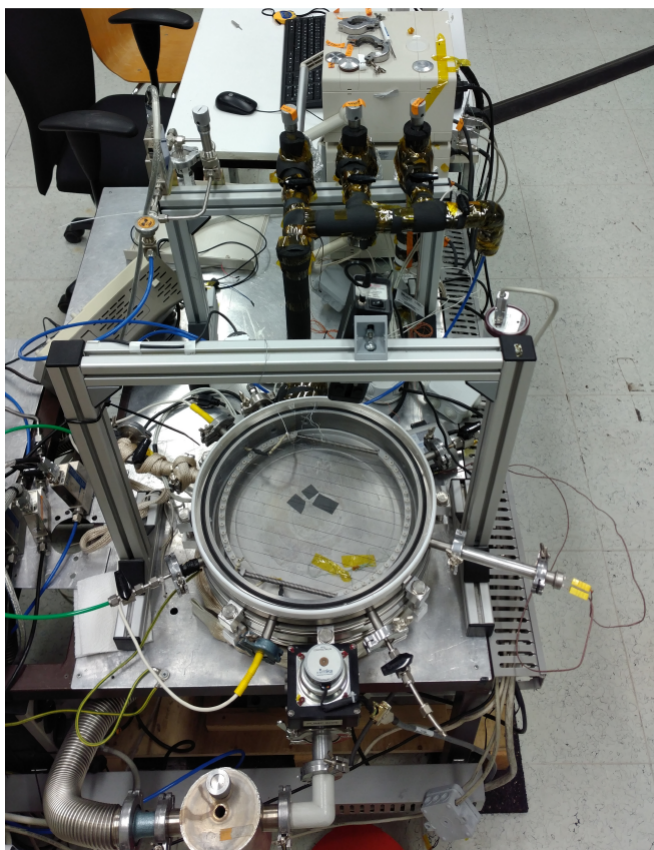


Figure 12: iCVD set-up at the Solid State Physics Institute at the Graz University of Technology

The main part of the iCVD set-up is a cylindrical vacuum chamber with a glass cover, which is evacuated by a rotary vane pump (PFEIFFER VACUUM DUO65) to a base pressure of around 1 mTorr. The substrate temperature is controlled by a chiller (THERMO SCIEN-

TIFIC ACCEL 500LC) connected to the bottom of the reactor, making substrate temperatures between 20 °C and 50 °C possible.

Chemical jars, which contain the chemicals for the experiment, are connected to the vacuum chamber via lines with needle valves. The jars are heated to controlled temperatures by a heater (OMEGA MCS-2110K-R) and supervised by a thermocouple, both connected to the chemical jar. The lines themselves are heated to about 100 °C to avoid condensation. During the iCVD process, the monomer vapours are led from the jars into the line system that feeds the gaseous components into the vacuum chamber. The needle valves are used to control the flow-rates of the evaporated chemicals flowing into the reactor. The initiator, which is kept at room temperature, has its own line leading into the chamber. The leak rate of the system as well as the flow-rates of the monomers are measured with a Labview-program, which drives a pressure control unit (MKS600 series pressure controller 651CD2S1N) connected to an electrically adjustable valve, that links the pump with the vacuum chamber of the reactor. The leak rate as well as the flow-rates are calculated by closing this valve and monitoring the pressure increase in time.

Hot nickel-chromium wires (Goodfellow, UK) inside the reactor near the glass lid on top are heated to about 250 °C by driving a current through them via a power supply (HEINZINGER PTN 350-5) to break apart the initiator molecules and to start the polymerisation process. The deposition itself is performed at a constant working pressure, usually between 200 mTorr and 350 mTorr.

The thickness of the growing polymer is controlled in-situ during the deposition using a He-Ne laser beam (633 nm ThorLabs), which is directed through the glass cover of the vacuum chamber onto a piece of Si wafer (Siegert Wafer, Germany) and reflected back into a detector, that measures intensity over time. The growing polymer layer on the Silicon results in an oscillating intensity at the detector. Taking the index of refraction (about 1.5), the incident angle of the laser (approx. 13°) and the laser wavelength into account, one can conclude that the thickness of the polymer increases by about 200 nm for each half period of the oscillating beam. Thus, the current thickness of the layer can be read from the intensity versus time graph by counting gaps between maxima and multiplying them by 200 nm, as shown in the example in fig. 13.

High accuracy is not needed as the thickness of the reference sample is measured after the deposition with ellipsometry (see sec. 8.1).

6.2 USED CHEMICALS

The following chemicals were used for the production of the examined samples. Their chemical structure is shown in fig. 14.

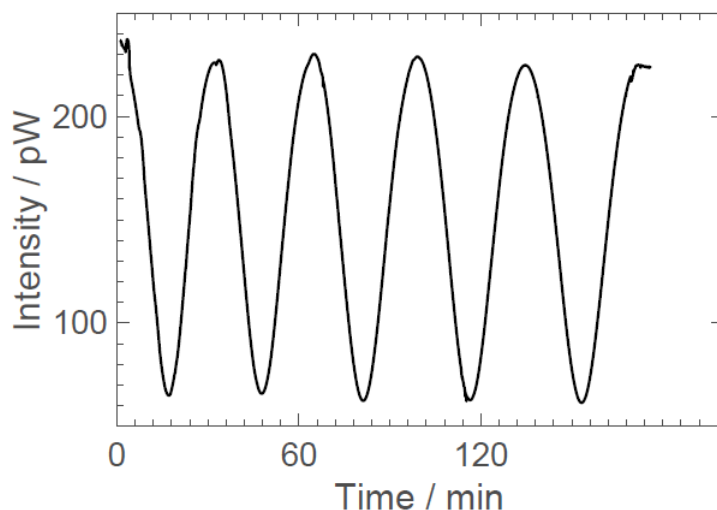


Figure 13: Graph demonstrating the in-situ thickness control for iCVD with a He-Ne laser

- *1-Allyl-3-methylimidazolium dicyanamide (AMID)* (98.5%, Sigma Aldrich): This specific ionic liquid was chosen because it exhibits high ionic conductivity and its chemical structure contains vinyl bonds, which are necessary for the iCVD polymerisation process (as described in sec. 4.4) to take place (for chemical structure see fig. 14c). As AMID was the only IL used for the described experiments, whenever the term "ionic liquid" (or short: "IL") is used thereafter in this thesis it is to be taken synonymously for "AMID", if not specified otherwise.
- *Ethylene glycol dimethacrylate (EGDMA)* (98%, Sigma Aldrich): This monomer was employed as a cross-linker to stabilise the obtained polymer films, resulting in a structure as shown in fig. 2 (for chemical structure see fig. 14d).
- *2-Hydroxyethyl methacrylate (HEMA)* (97%, Sigma Aldrich): HEMA is a hydrophilic monomer, which was chosen due to its specific molecular size. For the polymerisation process proposed in sec. 4.4 it was important to choose a monomer small enough to be able to partly diffuse into the ionic liquid, but big enough to lead to connected, stable films (for chemical structure see fig. 14b).
- *Tert-butyl peroxide (TBPO)* (98%, Sigma Aldrich): TBPO functions as an initiator. Its labile O-O-bond is broken by temperatures higher than 200 °C at the filament in the iCVD reactor in order to produce radicals initiating polymerisation (for chemical structure see fig. 14a).

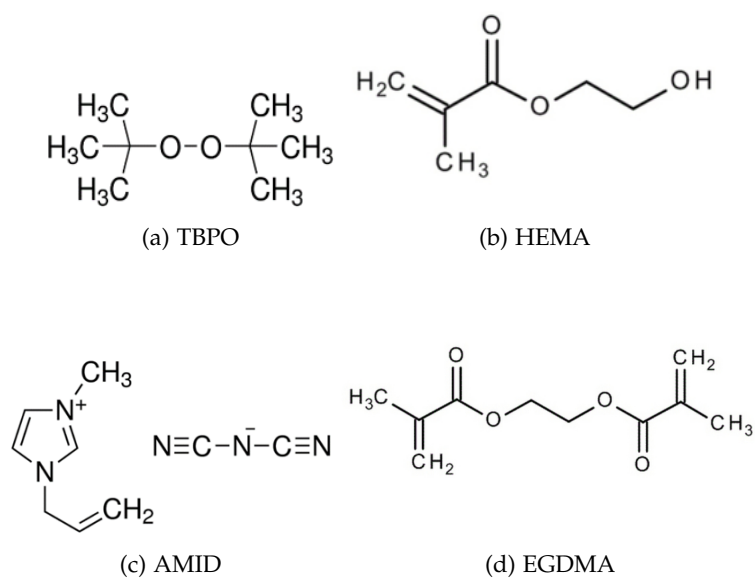


Figure 14: Chemicals used for sample production as detailed in sec. 6.2.

SAMPLE PREPARATION

The produced samples can roughly be divided into two types (as shown in fig. 15): Samples with pre-treated substrates and samples without pre-treated substrates. For the prior, the chosen substrate was pre-treated in some way before the liquid IL was transferred onto the substrate. After the IL was put onto the substrate it was solidified by depositing a *top-coating* with iCVD. The following sub-chapter will break the process of the sample production apart into single steps to illustrate the process.

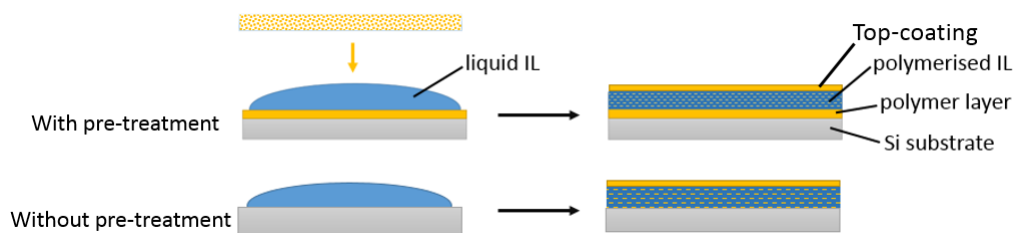


Figure 15: Schematic sample set-up. The produced samples can be roughly divided into two types: With pre-treatment of the substrate and without pre-treatment of the substrate.

7.1 SUBSTRATES AND THEIR PRE-TREATMENT

All samples were prepared on one of two types of substrates:

- *Si wafers*: Samples obtained on Si allowed for optical measurements such as spectroscopic methods (FTIR, spectroscopic ellipsometry).
- *Printed Circuit Boards (PCBs)*: The second type of substrates employed were custom-made PCBs, as depicted in fig. 16. The PCBs consist of a plastic base with copper electrodes covered by a thin gold layer on top (height of the electrodes: $36\ \mu\text{m}$). The electrodes have a specific distance from each other, that varies from electrode to electrode and ranges from 0.4 mm to 1.6 mm. The variation in distance allows to compare and verify the validity of resistivity measurements by checking the linear relationship of resistance versus distance. The green sticker on one side of the PCB protects part of the electrodes during sample preparation. When the PCB is used for resistivity measurements, the sticker is peeled off to connect the measurement device to the

revealed, clean electrode ends. Samples obtained on those substrates were mainly employed in topographical measurements and resistivity measurements using profilometry and EIS respectively.

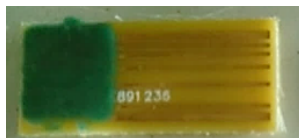


Figure 16: Custom made printed circuit board as described in sec. 7.1.

If the substrate was not pre-treated, liquid IL was directly transferred onto the naked Si wafer or the PCB in one of the ways described in sec. 7.2. However, often different pre-treatments were employed. Many were quickly discarded for not yielding a continuous solidified IL layer at the end of the process. Unsuccessful pre-treatments include using Si wafers which were pre-coated with ZnO, as the results show (see sec. 9.2.1).

A pre-treatment which was often employed as it showed favourable results (see sec. 9.2) was pre-coating both substrate types with a p(HEMA-EGDMA)-layer of 50 nm to 200 nm thickness via iCVD. The effect of various pre-coatings on the spreading of IL on the substrate was investigated with dynamic contact angle measurements (see sec. 9.2.1). Tab. 3 details the deposition parameters used for the pre-coatings. During the iCVD process the working pressure was always kept at 200 mTorr, the substrate temperature at 30 °C. The first depositions (no. 1 to no. 4) were solely performed to find a recipe for a stable polymer layer, whose composition is discussed in sec. 9.1.

7.2 TRANSFERRING IONIC LIQUID ONTO THE SUBSTRATE

The liquid IL was transferred onto the naked or pre-treated substrate in various ways. The aim was to achieve a continuous, homogeneous layer. Many deposition methods such as spin-coating or mixing the IL with solvents (e.g. iso-propanol or pure water) before drop-casting onto the substrate proved unsuccessful, since those led to multiple small droplets instead of a continuous layer or hindered the spreading of the IL respectively (see fig. 29).

Therefore, the method mainly employed was to drop-cast liquid IL onto the substrate with a pipette, either pure or mixed with liquid HEMA in different ratios. At the start of the experiments the amount of IL drop-cast was varied. However, it was soon found that an amount of 5-10 μ l worked best for the size of the employed substrates (approx. 2 \times 2 cm). Details on the transfer of liquid IL onto the substrates can be found in tab. 4. All samples marked with the addi-

Table 3: Pre-coating depositions via iCVD

No. ... number of deposition

t... thickness of resulting polymer film measured with ellipsometry

No.	sample names	flow-rates [sccm]			t [nm]
		TBPO	HEMA	EGDMA	
1	10.3-Si1-8	0.74	0.42	0.05	197
2	10.3-Si9	0.75	0.74	0.11	211
3	14.3-Si1	0.75	0.82	0.08	221
4	14.3-Si2	0.74	0.80	0.17	218
5	14.3-Si3-8	0.74	0.80	0.15	212
10	13.4-PCB1-3	0.75	0.73	0.13	223
12	25.4-Si1-6 + -PCB1-6	0.79	0.73	0.17	182
15	18.5-PCB1-6	0.74	0.54	0.14	50
18	20.6-Si1-5	0.72	0.46	0.11	207
19	22.6-Si1-3 + -PCB1-6	0.78	0.75	0.11	74
21	3.7PCB1-6	0.78	0.62	0.12	67
24	10.7-PCB1-9	0.77	0.66	0.14	70
28	5.9-Si1-5 + -PCB1-6	0.78	0.70	0.10	62
31	13.11-Si1-5	0.76	0.70	0.17	50
32	14.11-Si1-8	0.76	0.59	0.12	50

tional note "J. Pilz" were received from this colleague and consisted of Si wafers coated with 14 nm ZnO by atomic layer deposition.

Table 4: Transfer of ionic liquid onto substrates

V... total amount of liquid deposited

type... type of liquid(s) deposited; if more than one liquid was used, the following numbers express the mixing ratio

method... method with which the liquid was transferred onto the substrate

sample name	V [μ l]	type	method
23.3-Si1	5	IL	drop-cast
23.3-Si2	10	IL	drop-cast
23.3-Si3	200	IL	drop-cast
28.3-Si1	2	IL	drop-cast
28.3-Si2	5	IL	drop-cast
28.3-Si3	10	IL	drop-cast
28.3-Si4	20	IL	drop-cast
29.3-Si1	2	IL	drop-cast
29.3-Si2	5	IL	drop-cast
29.3-Si3	10	IL	drop-cast
29.3-Si4	20	IL	drop-cast
14.3-Si2	2	IL	drop-cast
14.3-Si4	5	IL	drop-cast
14.3-Si6	10	IL	drop-cast
14.3-Si7	20	IL	drop-cast
13.4-PCB1	2	IL	drop-cast
13.4-PCB2	5	IL	drop-cast
13.4-PCB3	10	IL	drop-cast
20.4-PCB1,4	2	IL	drop-cast
20.4-PCB2,5	5	IL	drop-cast
20.4-PCB3,6	10	IL	drop-cast
25.4-PCB1,4	2	IL	drop-cast
25.4-PCB2,5	5	IL	drop-cast
25.4-PCB3,6	10	IL	drop-cast
27.4-PCB1,4	2	IL	drop-cast
27.4-PCB2,5	5	IL	drop-cast
27.4-PCB3,6	10	IL	drop-cast
25.4-Si1	2	IL	drop-cast
25.4-Si2	5	IL	drop-cast
25.4-Si3	10	IL	drop-cast

Table 4: Continued: Transfer of ionic liquid onto substrates

sample name	V [μ l]	type	method
25.4-Si4	20	IL	drop-cast
18.5-PCB1-3	10	IL	drop-cast
18.5-PCB4-6	10	IL	drop-cast
20.6-PCB1,2	5	IL	drop-cast
20.6-Si1	2	IL	drop-cast
20.6-Si2	10	IL	drop-cast
22.6-PCB1,2	5	IL	drop-cast
22.6-Si1	10	IL	drop-cast
22.6-Si1	2	IL	drop-cast
3.7-PCB1-3	5	IL	drop-cast
3.7-PCB4-6	5	IL	drop-cast
10.7-PCB1-2	5	HEMA:IL - 1:2	drop-cast
10.7-PCB3-4	5	HEMA:IL - 1:10	drop-cast
10.7-PCB5-8	5	(HEMA:IL) 1:20	drop-cast
Dep41-Si1,2 (J. Pilz)	10	IL	drop-cast
Dep41-Si3 (J. Pilz)	100	IL	spin-coated
5.9-PCB1,2 + -Si4	100	IL	drop-cast
24.10-Si1,3,5	10	IL	drop-cast
13.11-Si1	5	HEMA:IL - 2:1	drop-cast
13.11-Si2	5	HEMA:IL - 5:1	drop-cast
13.11-Si3	5	HEMA:IL - 10:1	drop-cast
13.11-Si1-5	5	HEMA:IL - 20:1	drop-cast
14.11-Si2	5	IL	drop-cast
14.11-Si3	5	HEMA:IL - 2:1	drop-cast
14.11-Si4	5	HEMA:IL - 5:1	drop-cast
14.11-Si5	5	HEMA:IL - 10:1	drop-cast
14.11-Si6	5	HEMA:IL - 20:1	drop-cast
14.11-Si7	5	IL	drop-cast
24.11-Si1-5	5	IL	drop-cast

7.3 POLYMERISING IONIC LIQUID VIA INITIATED CHEMICAL VAPOUR DEPOSITION

After transferring the liquid IL onto the substrate, it was solidified via depositing a p(HEMA-EGDMA)-film on top (= "top-coating") via iCVD. For the procedure the substrate temperature was always kept at 30 °C, the working pressure at 200 mTorr. To aid the diffusion

of HEMA into the IL, prior to heating the filament (and thus prior to the polymerisation process), the HEMA line was opened in various cases at working pressure and HEMA was flown into the reaction chamber. This process is termed *HEMA pre-flow*. Tab. 5 gives the deposition parameters for the solidification of IL via iCVD including the time of HEMA pre-flow. Obtained thicknesses of the p(HEMA-EGDMA) coating for solidifying the IL lie between 400 nm and 800 nm (exact values were measured via ellipsometry).

The state of the finished sample were investigated with the characterisation techniques detailed in sec. 8.

Table 5: iCVD coatings performed to solidify IL

No. ... number of deposition

t... thickness of resulting polymer film measured with ellipsometry

t_{p-f}... duration of HEMA pre-flow before deposition

No.	sample	t _{p-f} [min]	TBPO	HEMA	EGDMA	t [nm]
flow-rates [sccm]						
6	23.3-Si1-3	30	0.75	0.56	0.13	200
7	28.3-Si1-4	30	0.68	0.67	0.10	465
8	29.3-Si1-4	10	0.76	0.67	0.14	461
9	14.3-Si2,4,6,7 + 13.4-PCB1-3	30	0.76	0.52	0.12	509
13	25.4-PCB1-3 + 27.4-PCB1-3	30	0.79	0.27	0.07	440
14	25.4-Si1-4 + -PCB4-6 + 27.4-PCB4-6	10	0.78	0.29	0.08	495
15	18.5-PCB1-3	30	0.76	0.51	0.16	430
16	18.5-PCB4-6	10	0.73	0.49	0.11	456
20	20.6-PCB1,2 + -Si1,2 + 22.6-PCB1,2 + -Si1,2	0	0.77	0.22	0.08	500
22	3.7-PCB1-3	10	0.77	0.35	0.12	845
23	3.7-PCB4-6	10	0.73	0.41	0.12	800
25	10.7-PCB1-4	0	0.76	0.29	0.11	419
26	10.7-PCB5-8	0	0.76	0.29	0.10	462
27	Dep41-1,2 (J. Pilz)	10	0.77	0.79	0.14	400
29	5.9-PCB1,2 +	10	0.76	0.40	0.11	433

Table 5: Continued: Coatings performed to solidify IL

No.	sample	t_{p-f} [min]	TBPO	HEMA	EGDMA	t [nm]
	-Si4 + Dep41-3 (J. Pilz)					
33	14.11-Si2-6	0	0.75	0,33	0.09	800
34	14.11-Si7 + 13.11-Si1-3,5	0	0.76	0.28	0.09	400

CHARACTERISATION TECHNIQUES

The obtained samples were characterised with the following techniques to gain insight into various properties of the solidified ionic liquid, such as surface topography, degree of polymerisation, resistivity and conductivity as well as the influence of tuned parameters during the sample preparation on the named properties. This chapter introduces the set-up and measurement principle of the employed techniques.

8.1 SPECTROSCOPIC ELLIPSOMETRY

Ellipsometry is a technique used to determine thickness, refractive index and roughness of thin films. For the experiments conducted for this thesis, ellipsometry was performed on Si substrates coated with polymer thin-films produced via iCVD to determine their thickness. A picture of the used ellipsometer (M-2000V, J.A. Woolam Co.Inc.) can be found in fig. 17.

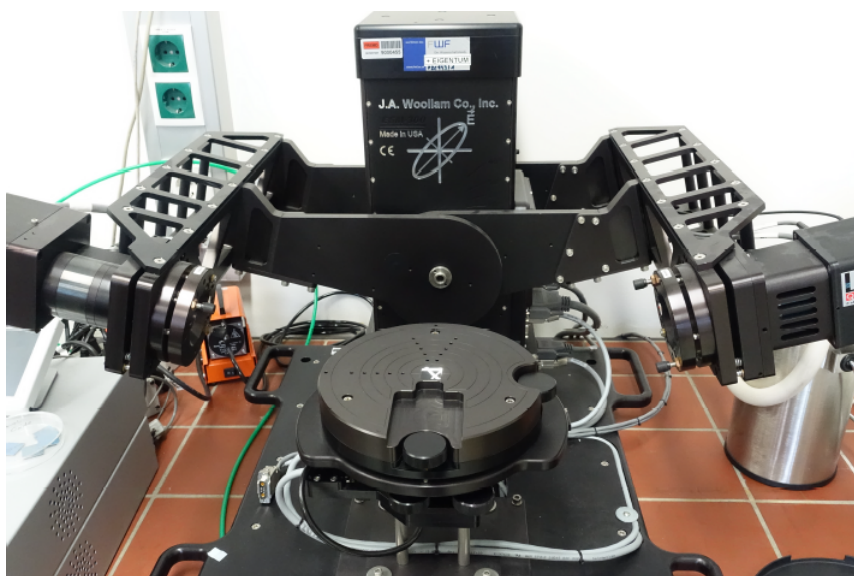


Figure 17: Ellipsometer used for ellipsometry measurements

For a measurement the sample is irradiated with linearly polarised light (wavelength in the range of 371-1000 nm, given by the measurement device). After interaction with the sample, the reflected beam has changed its polarisation depending on the film properties and its thickness. This change in polarisation is measured and parameterised by the amplitude ration and the phase difference. In the following

equation, r_p and r_s describe the Fresnel reflection coefficients for the p- and s-polarised light:

$$\frac{r_p}{r_s} = \tan(\Psi)e^{i\Delta} \quad (6)$$

The reflected spectrum can be measured for several incident angles [28].

The obtained data was fitted by the software Complete EASE. One has to apply a physically sensible optical model for the analysed films. To determine the thickness of the p(HEMA-EGDMA) polymer films, a Cauchy-model was employed. The refractive index in the Cauchy-model is

$$n(\lambda) = A + \frac{B}{\lambda^2} + \frac{C}{\lambda^4} \quad (7)$$

where n stands for the wavelength-dependent refractive index, λ for the wavelength and A , B and C are fit parameters [29]. For thickness determination a three angle measurement was performed at 65, 70 and 75 degrees. To simulate the investigated samples a silicon substrate, a 1.7 mm SiO_2 on top and a Cauchy layer for transparent polymer film on top was modelled in the program.

8.2 DYNAMIC CONTACT ANGLE MEASUREMENTS (DCAM)

The contact angle Θ_c measures how well a liquid wets a solid surface. It is geometrically defined as the angle formed by a liquid at the three phase boundary where a liquid, gas and solid intersect. The balance at the three phase contact is described by the Young equation, which thus also gives the contact angle Θ_c :

$$\gamma_{SG} - \gamma_{SL} - \gamma_{LG} \cos(\Theta_c) = 0 \quad (8)$$

where γ_{SG} , γ_{SL} and γ_{LG} represent the inter-facial tensions, which form the equilibrium contact angle of wetting. This is further illustrated in fig. 18. A low contact angle (lower than 90°) indicates that the liquid spreads on the surface, while high contact angle values show poor spreading.

Static contact angles are measured when the droplet is standing on the surface and the three phase boundary is not moving. In contrast, dynamic contact angle measurements (dCAM) are used as the three phase boundary moves [30]. These measurements consist of two phases: first an ever growing drop of the liquid is deposited onto the substrate surface and a so called *advancing angle* is measured at every step. The second phase is to measure the *receding angle*. For this, the drop is gradually sucked back into the syringe. The receding angle is

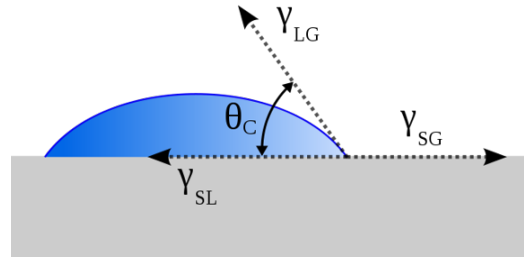


Figure 18: Depiction of the principle of contact angle measurements as detailed in se.8.2

obtained at the moment right before the three phase boundary starts to move. This means, that one can obtain many advancing angles but only one receding angle with one dCAM measurement. For statistical purposes, this procedure is repeated multiple times. Advancing and receding contact angles give the maximum and minimum values the static contact angle can have on the surface; thus the differences between the two can be very high [30]. All contact angle measurements performed for this thesis were dCAM measurements conducted with an optical contact angle meter (KSV INSTRUMENTS LTD, Cam200) and evaluated with the software CAM2008.

8.3 PROFILOMETRY

Profilometry is a technique commonly used to measure height differences and to obtain one dimensional height profiles. All profilometers include a detector and a sample stage in their set-up. The detector determines where the points of the sample are and the sample stage holds the sample. Either the sample stage or the detector moves to allow for measurement.

There are two types of profilometers: Stylus and optical. Stylus profilometers physically move a tip along the surface of the sample in order to acquire the surface height. This is done mechanically with a feedback loop that monitors the force from the sample pushing up against the tip as it scans along the surface. When the surface height changes, the system also adjusts the height of the tip to keep the force constant. The changes in the Z-position of the arm holder can then be used to reconstruct the surface [31].

For this thesis, profilometry was used to gain insight into the homogeneity and topography of the solidified IL-films. The height of the layer was also of importance for conductivity calculations of the obtained layers after eq. 5. Measurements were conducted with a BRUKER DektakXT, as depicted in fig. 19 and performed with a constant force of 3 mg, over a length of 15000 μm and an acquisition time of 1 min. The measurements were controlled via the computer program Vision64.

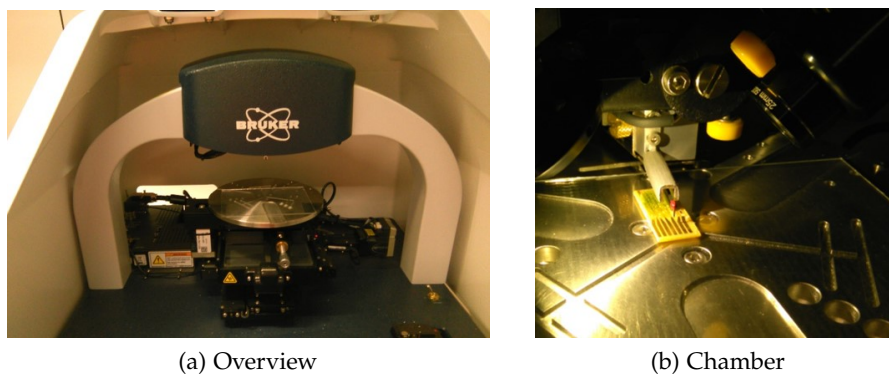


Figure 19: Profilometer used for the measurements: An overview (left) and a closer look at the measurement chamber (right)

8.4 FOURIER TRANSFORM INFRARED SPECTROSCOPY (FTIR)

Fourier transform infrared spectroscopy (FTIR) induces stretching and bending modes of molecules by using infrared light, leading to absorption of the light at specific wavelengths. The Michelson-interferometer divides an infra-red beam into two parts via a beam splitter and then recombines them again after a path difference has been introduced (usually by a moving mirror). Due to the path difference, interference occurs. The variation in intensity as a function of the path difference yields the spectral information. The modulated beam then leaves the interferometer, passes through a sample cell and is focused on a detector. A computer performs a Fourier transform of the measured interferogram, providing a single-beam spectrum [32].

For this thesis a Michelson-interferometer (Bruker IFS 66V) was used to gain information on the chemical state and composition of the obtained films. The measurement environment was kept under vacuum to minimise light scattering. Before measuring the film, the naked substrate was measured. The obtained spectrum for the polymer film was divided by this substrate reference spectrum. To get information of the solidified IL only, also reference samples with p(HEMA-EGDMA) films were measured separately to divide them from the sample with solidified IL in order to gain information of the IL-layer only.

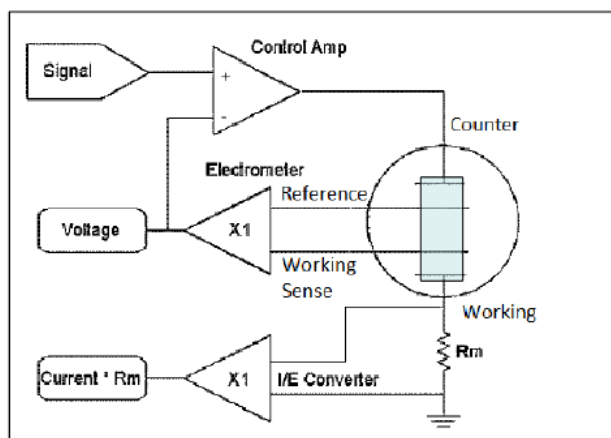
8.5 ELECTROCHEMICAL IMPEDANCE SPECTROSCOPY (EIS)

The fundamental concept behind electrochemical impedance spectroscopy (EIS) has already been explained in sec. 5. For the measurements a REFERENCE 600 from Gamry Instrument was utilised. The device as well as its working principle are depicted in fig. 20.

The user defines a signal (voltage over time) which is then generated by the device. The signal moves to the control amplifier, which



(a) Device



(b) Working Principle

Figure 20: Measurement device employed for the EIS measurements (left) and its working principle (right).

controls its output such that the feedback voltage equals the signal at its negative input. The feedback voltage, which is the voltage between the reference and the working sense electrode is measured. This seems redundant but the information can be used to check whether the control amplifier works correctly. The resulting current is then measured at the shunt resistor, R_m .

To measure the conductivity of solidified IL custom built printed circuit boards (PCBs), such as shown in fig. 16, were coated with solidified IL as described in sec. 7. The PCB was inserted into a counterpart plug, that could easily be connected to the REFERENCE 600 via the measurement clamps of the device. For two-point measurements working and working sense electrode were connected to one electrode, counter and reference to the other. All resistivity measurements were performed as two-point potentiostatic EIS measurements in ambient air. Since the measurements were performed in low humidity conditions, a two-point set-up could be utilised without sacrificing accuracy for the measured values (further explained in sec. 5.2).

Part III

RESULTS AND DISCUSSION

This part presents and discusses the obtained results. Conclusions are drawn on how the tuned experimental parameters influence polymerisation, homogeneity and conductivity of the samples.

TUNING DEPOSITION PARAMETERS

Various deposition parameters were varied to find an optimum recipe for solidifying IL via iCVD. The effect of changed parameters on topography and polymerisation of the IL was investigated with dCAM, Profilometry as well as FTIR.

9.1 STABLE POLYMER FILMS

For pre-coating the employed substrates as well as the solidification of liquid IL with a p(HEMA-EGDMA) thin film it was of great importance to produce stable polymer films. The first depositions were solely performed to find out which flow-rate ratio of initiator, monomer and cross-linker would result in a layer stable against water (as noted in sec.7.1). The thickness of the resulting iCVD thin films was measured with ellipsometry before and after rinsing the sample surface with purified water. The flow-rate composition was changed until no thickness change occurred between the measurements before and after water, resulting in the flow-rates of deposition⁴ in tab. 3.

With the help of the program "IR_fitter" written by M. Tazreiter (freely available on github¹) the composition of the obtained stable polymer films could be determined. To use the program, one has to do FTIR measurements of the single spectra (in our case HEMA and EGDMA) as well as a spectrum of the co-polymer film. When loading all spectra into the IR_fitter, the amount of each monomer in the co-polymer film is determined with a Bouguer-Lambert-Beer approximation after correcting the baseline of all absorbance spectra [33]. The resulting graph is shown in fig. 21 and the obtained percentage for each homomer resulted in 9.5 % EGDMA and 90.5 % HEMA.

9.2 EFFECT OF PRE-COATING ON UNIFORMITY OF LAYERS

Profilometry and dCAM measurements were performed to study the effect of various pre-coatings on the spreading of the liquid IL on the substrate, the wetting of the substrate and the homogeneity of the resulting layers of solidified IL.

¹ https://github.com/MartinTa/IR_fitter

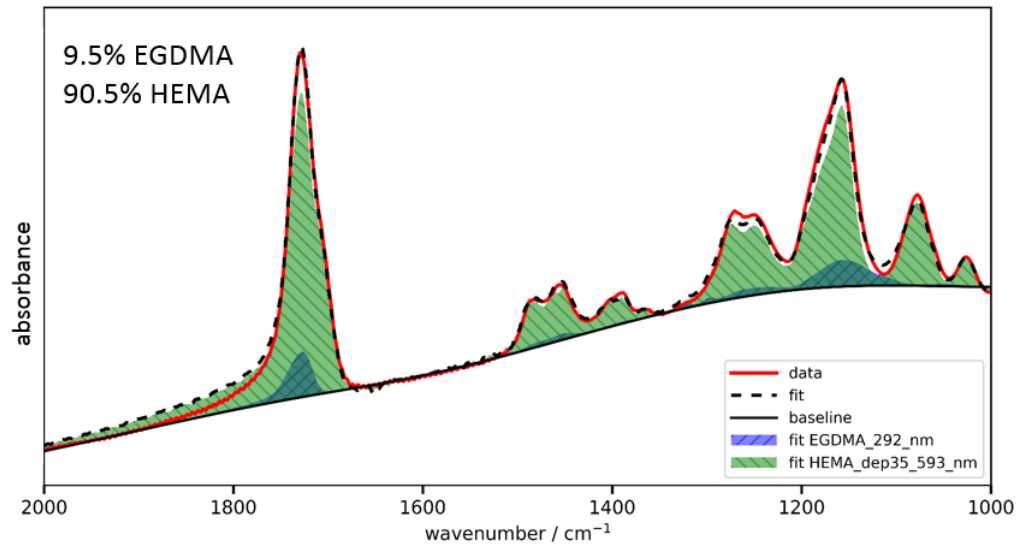


Figure 21: Determining the composition of the stable HEMA-EGDMA copolymer film with the IR_fitter software

9.2.1 Dynamic Contact Angle Measurements

The wetting of various pre-coatings with liquid IL was investigated via dynamic contact angle measurements as detailed in sec. 8.2. As can be seen from the results, depicted in fig. 22, the investigated substrates behave quite differently from each other. Also the advancing contact angles and the receding contact angles differ significantly from each other for each measured substrate. The higher advancing contact angles can be attributed to the large viscosity of the IL, which leads to very slow spreading. Since the receding contact angle allows better insight in the adhesion of the liquid IL to the substrate surface than the advancing angle, the values of the former are of more importance. When looking at the results for the receding contact angle, although all values are now smaller than the respective advancing angles, it becomes clear that a pre-coating with p(HEMA-EGDMA) yields the best results for wetting of the surface. The hydrophilic polymer coating binds the liquid IL to the substrate best. Therefore pre-coating the substrate with this co-polymer is deemed favourable.

9.2.2 Profilometry

The surface topography of the samples was investigated with profilometry. Fig. 23 presents results from profilometry measurements performed on differently prepared substrates. The picture shows three profilometry height profiles of solidified IL measured between two electrodes of PCBs. The red curve shows the measurement of solidified IL on a naked substrate, the blue curve a measurement of solidified IL on a substrate that was pre-coated with 50 nm p(HEMA-

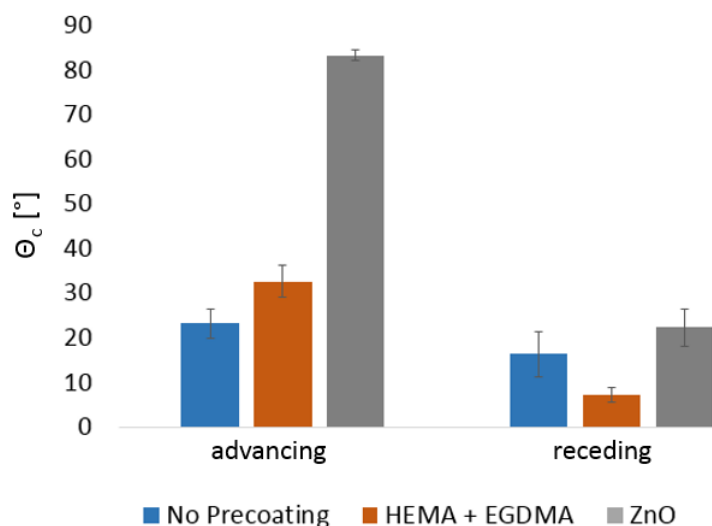


Figure 22: Results of dynamic contact angle measurements performed with liquid IL on various substrates

EGDMA) and the black curve shows a measurement on a substrate that was pre-coated with 200 nm p(HEMA-EGDMA). From comparing the curves, it becomes obvious that the IL spreads better the thicker the p(HEMA-EGDMA) pre-coating layer gets.

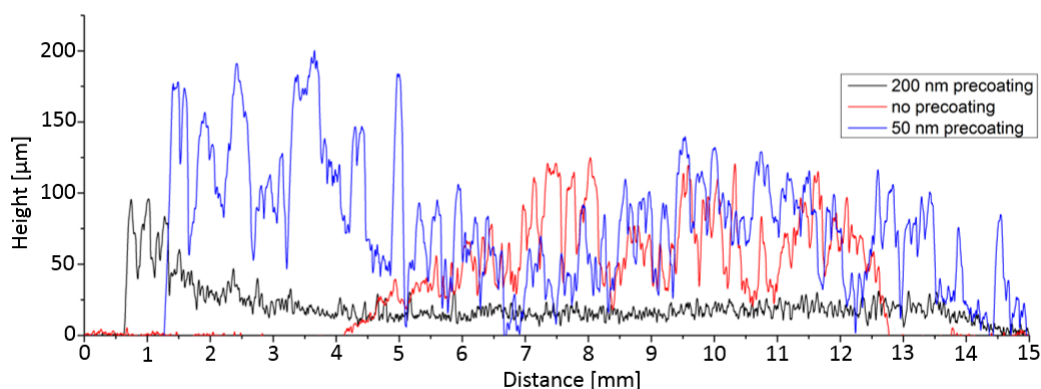


Figure 23: Profilometry measurements of solidified IL showing that pre-coating of the substrates with p(HEMA-EGDMA) aids spreading and uniformity of the resulting film.

Depositing the liquid IL onto a non-pre-coated substrate results in a localized, very rough, uneven drop of solidified IL. The substrate pre-coated with 50 nm p(HEMA-EGDMA) already leads to more favourable results, indicating that the pre-coating aids the spreading of the liquid although the layer still shows large thickness-variations and appears rough. The black curve, which shows the sample that was pre-coated with 200 nm p(HEMA-EGDMA) shows a quite homogeneous layer of solidified IL that is spread over the whole

substrate and shows roughly the same thickness along the measured length.

Before performing the profilometry measurements on the PCBs the green sticker on them was pulled off to get a reference height of zero for the measurements (visible on the very left for all curves in fig. 23). The rise in thickness to the left in the blue and black curves can be attributed to the presence of the sticker during sample preparation: During the iCVD deposition, the IL was partly "pushed" towards the edge of the sticker, where it could not spread further, before solidifying. Therefore, the layer is thicker near the previous location of the edge of the sticker.

Together with the results from the dCAM measurements (sec. 9.2.1) it can be concluded that pre-coating substrates with a co-polymer consisting of HEMA and EGDMA in the stable composition presented in sec. 9.1 aids the spreading of liquid IL on the substrate and results in more homogeneous films of solidified IL.

9.3 INVESTIGATING THE DEGREE OF POLYMERISATION

The state of polymerisation of the solidified IL was investigated via FTIR. Fig. 24 compares the FTIR spectra of p(HEMA-EGDMA) and liquid IL with a spectrum of solidified IL. The black spectrum represents the liquid IL, whose chemical structure is depicted in fig. 14c. The spectrum clearly shows the C=C stretching of the whole bond at around 1650 cm^{-1} and other stretchings occurring in the vinyl bonds ranging from 3150 cm^{-1} to around 3000 cm^{-1} . The two peaks at 3100 cm^{-1} and a little above 3000 cm^{-1} show the antisymmetric stretching of CH in the CH_2 -bond and the CH symmetric stretching in the CH_2 -bond at the vinyl bond of the liquid IL. Since the vinyl bonds are still partly visible in the solidified IL (represented by the red curve in fig. 24), we can conclude that the ionic liquid was not completely polymerised by the iCVD process. The fact that the IL is completely solidified - so well, that it could be pulled off from the substrate in instances to obtain a free standing membrane of solidified IL (see fig. 25) - however, indicates that the IL has to be at least partly polymerised by the process. This strengthens the claim on the polymerisation mechanism proposed in sec. 4.4. Also the fact, that the $\text{C} \equiv \text{N}$ bonds are still clearly visible is a good sign, since this bond only occurs in the counter ion which should not be altered in order to stay mobile and still be conductive in the solid IL-layer.

To investigate the effect of various deposition parameters on the degree of polymerisation, samples with different deposition parameters were prepared and compared to each other via FTIR. The effect of the following parameters on the polymerisation of the IL was investigated:

- Amount of liquid IL drop-cast

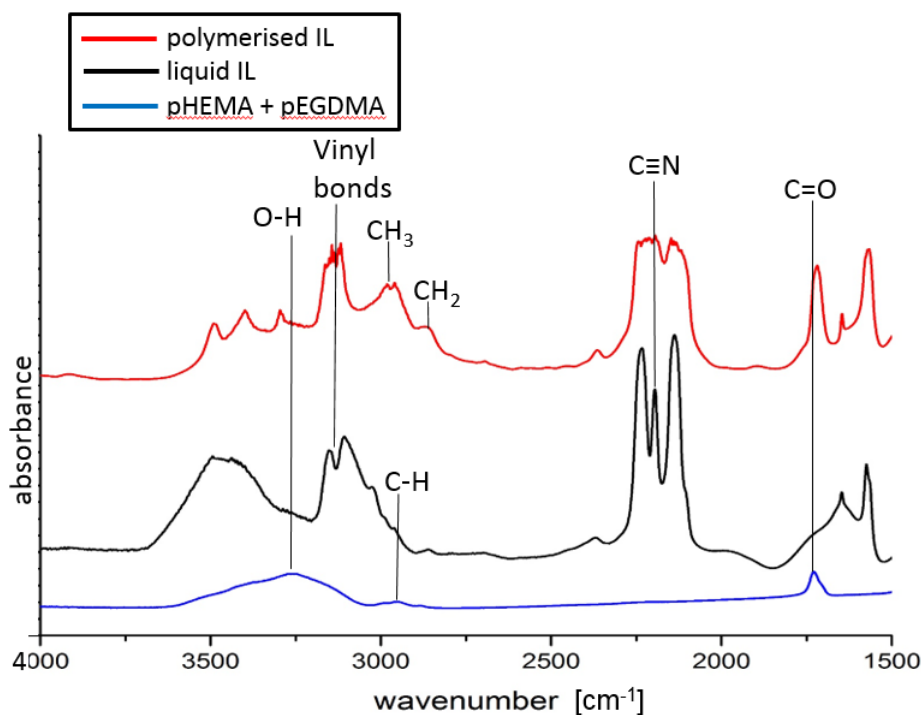


Figure 24: Comparing FTIR spectra of liquid IL, solid IL and p(HEMA-EGDMA) co-polymer

- Duration of HEMA pre-flow
- Thickness of top-coating
- Drop-casting pure IL vs. drop-casting liquid IL mixed with liquid HEMA
- Pre-coating the substrate vs. no pre-coating

The obtained results are visible in fig. 26 and fig. 27. Fig. 26a shows the results for drop-casting pure IL vs. IL mixed with HEMA. Tuning this parameter yields no visible effect on the degree of polymerisation, which is curious, since one would naively assume that mixing HEMA with IL in both their liquid state would lead to better polymerisation since the HEMA "diffuses" deeper into the IL. The large shoulder visible in this spectra at around 3600 cm^{-1} to 3200 cm^{-1} is an artefact of the detector. Also, changing the thickness of the top-coating (depicted in fig. 26b) as well as changing the amount of liquid IL which was drop-cast on the substrate (see fig. 27a) and the duration of HEMA-pre-flow prior to the polymerisation process (fig. 27b), did not lead to visibly differing results. Still, a minimum time of HEMA pre-flow had to be employed during the iCVD process since the liquid IL would not solidify otherwise as shown in the example in fig. 28.

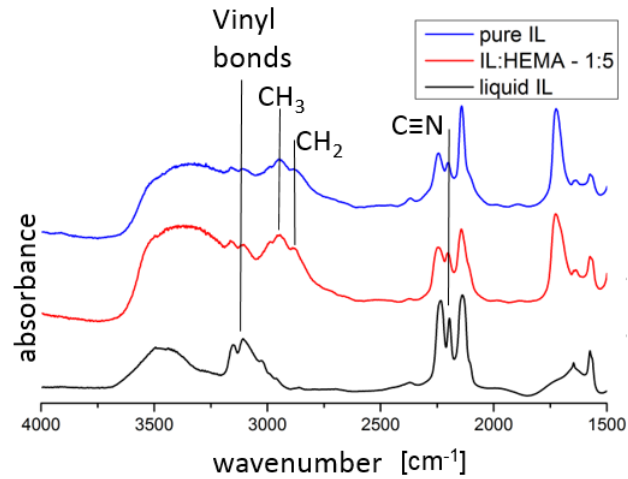
When comparing fig. 27a with fig. 27b one can spot differences at the peaks representing the vinyl bonds of the IL. The samples



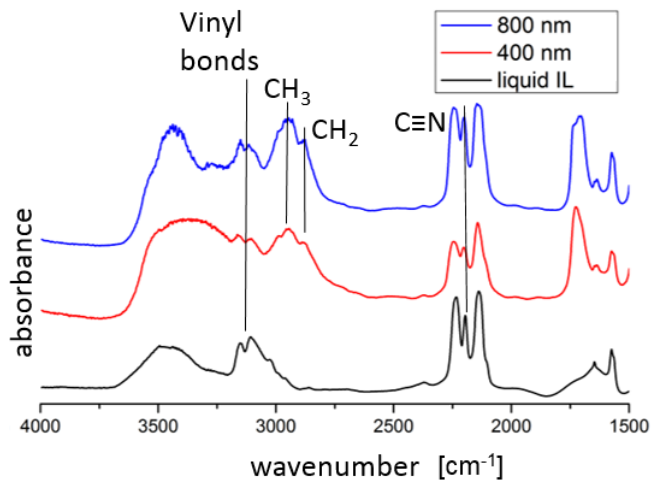
Figure 25: Si substrate pre-coated with p(HEMA-EGDMA), drop-cast with IL which was solidified in another iCVD process. The solidified IL starts to detach from the substrate (left) and can be pulled off to gain free-standing membranes (right).

in fig. 27a were not pre-coated whereas those in fig. 27b were (with p(HEMA-pEGDMA) films). The peak which corresponds to the C-H symmetric stretching in the CH_2 bond is not visible for the pre-coated samples. No quantitative statements can be made from observing the spectra but comparatively the effect is visible.

With this we can conclude from the FTIR measurements that pre-coating the substrate with p(HEMA-EGDMA) also aids the polymerisation. Furthermore, the measurements show that the IL was only partly polymerised and that many parameters such as which amount of IL was drop-cast, drop-casting pure IL vs. IL mixed with liquid HEMA, the duration of the HEMA-pre-flow and thickness of the top-coating do not seem to play a role in the polymerisation process.

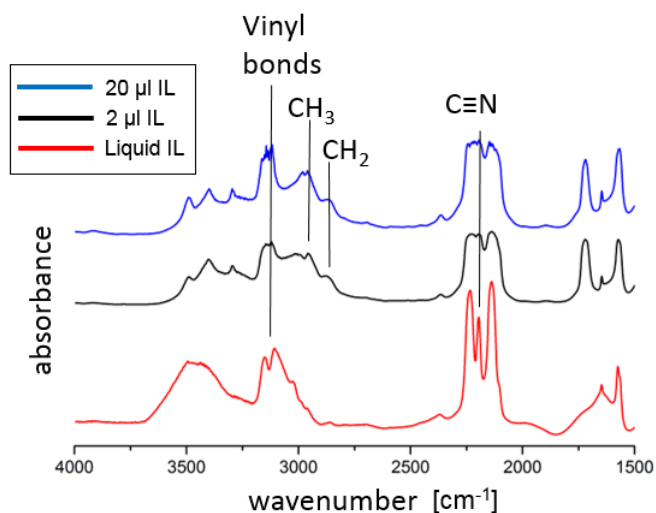


(a) Dropcasting IL vs. IL+HEMA

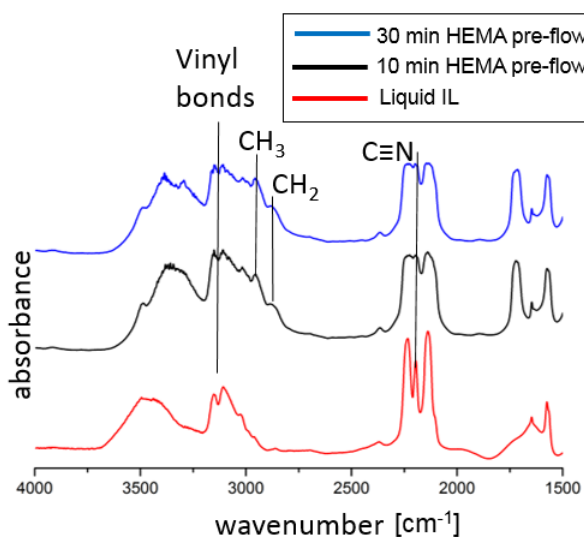


(b) Varying top coating thickness

Figure 26: Comparing FTIR spectra of solidified IL deposited with varying deposition parameters to gain insight on the effect of those parameters on the degree of polymerisation of the solidified IL



(a) Varying amount of IL dropcast (measurement on non-pre-coated substrates)



(b) Varying HEMA pre-flow time (measurement on pre-coated substrates)

Figure 27: Comparing FTIR spectra of solidified IL deposited with varying deposition parameters to gain insight on the effect of those parameters on the degree of polymerisation of the solidified IL

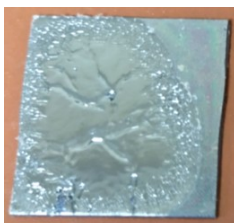


Figure 28: IL film after depositing a top-coating without employing a HEMA pre-flow. The drop is not completely solidified.

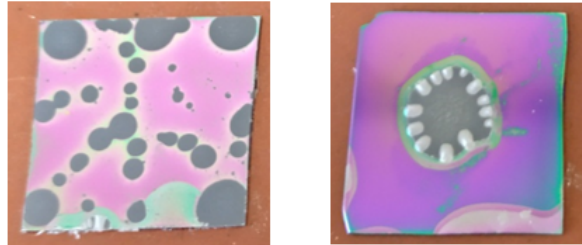


Figure 29: Undesired effects when transferring IL onto the substrate: Spin-coating IL onto a substrate (left) leads to disrupted layers (continuous layers desired) and depositing the IL with various solvents (e.g. pure water, on the right) hinders spreading of the layer.

RESISTIVITY AND CONDUCTIVITY

10.1 FITTING MODELS FOR RESISTIVITY RESULTS

The resistivity of solidified IL was measured on PCBs with EIS as explained in sec.8.5 by fitting appropriate electrical circuits onto the obtained data. Fig. 30 shows the models employed for the measurements. Fig. 30a depicts the model that was used for fitting the samples obtained from non-pre-coated substrates whereas the model depicted in fig. 30b is the one employed for samples whose substrates were pre-coated.

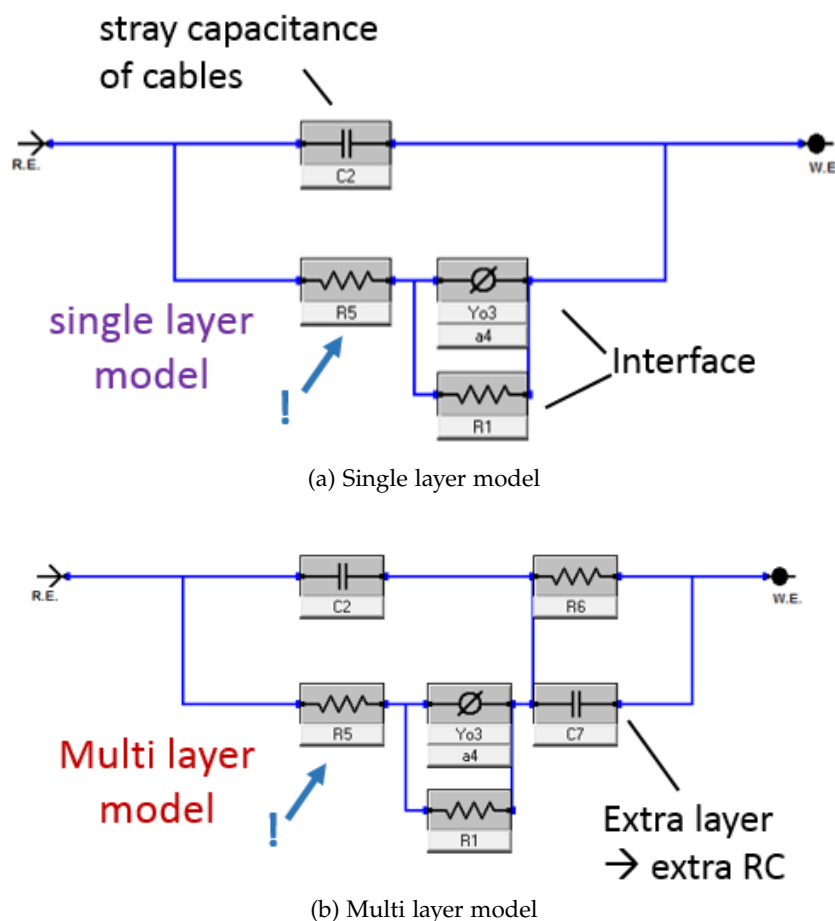
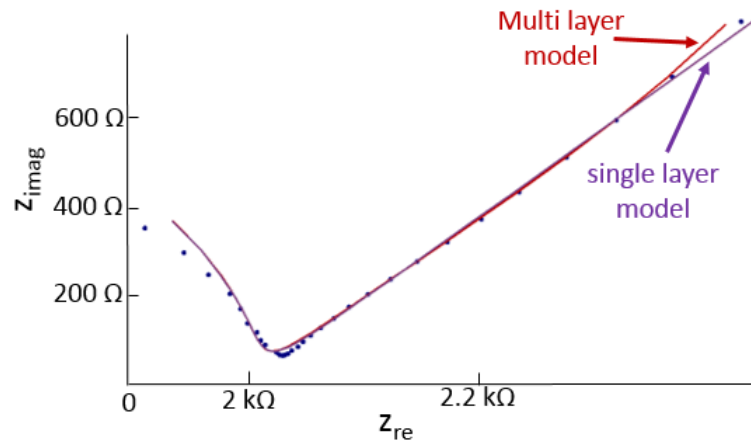


Figure 30: Fitting models used to describe the data obtained by EIS and thus obtain the resistance R_5 of the solidified IL membrane.

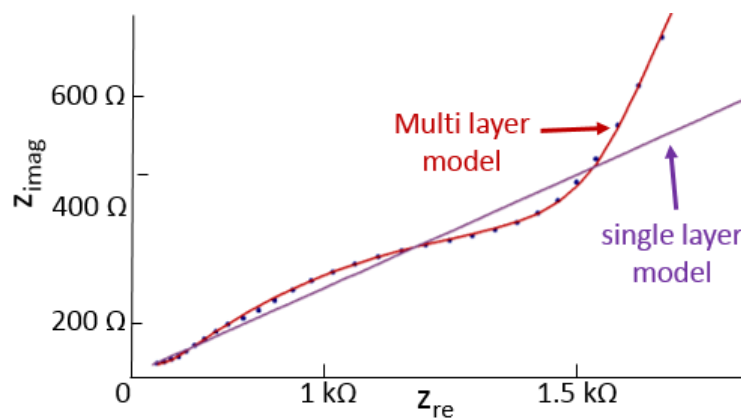
In both models, the capacitance C_2 represents the stray capacitance of the cables in the measurement set-up. The constant phase element and R_1 in parallel represent the interface between the electrodes and

the solidified IL. The resistance of the solid electrolyte is noted as R_5 in the drawing of the model and this is the resistance which is obtained by the fit. The multi layer model contains an extra RC to compensate for the extra polymer layer between the electrodes on the substrate and the solidified IL, which we want to measure.

Fig. 31 illustrates how each model works best for its intended purposes. The non-pre-coated sample in fig. 31a shows similar results for both of the models over a large part of the measurement curve. But we can see that the behaviour of the two models start to differ on the right side of the curve and that the single layer model describes the curve better than the multi layer model. This makes sense, since the multi layer model assumes an additional layer in the sample, which is not present in this case. When we look at the example in fig. 31b which depicts a pre-coated sample, we see that the multi layer model describes the measured data much better than the single layer model. the single layer model misses the representation of the pre-coating and thus is useless in this case.



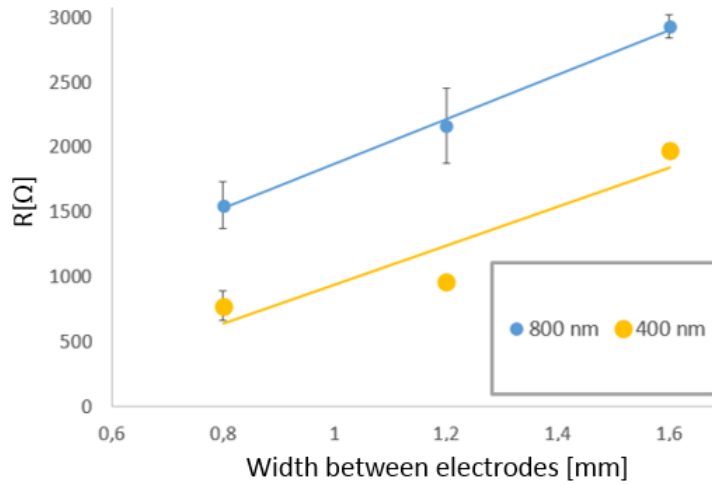
(a) Non-pre-coated sample



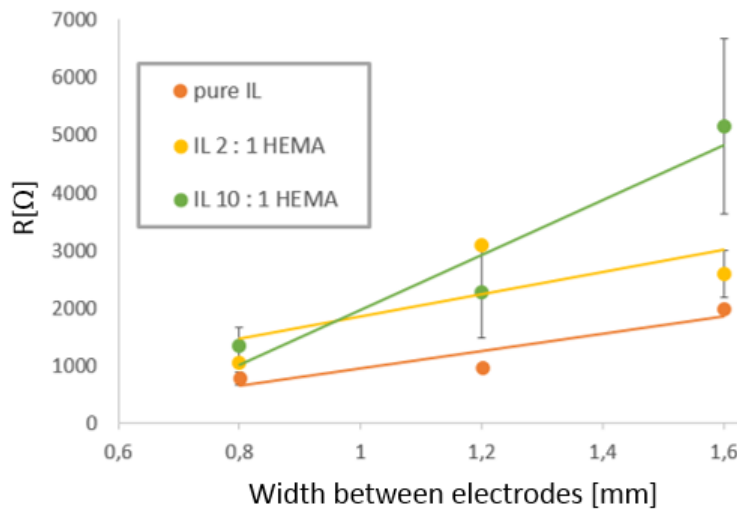
(b) Pre-coated sample

Figure 31: Fitting models of fig. 30 employed on EIS measurements (depicted as Nyquist-curves) on a non-pre-coated and a pre-coated sample.

One way to ensure the validity of the chosen models for fitting resistivity data is to measure the resistance on one sample over varying distances (as explained in sec. 7.1). A measured resistance which rises linearly with the distance between the electrodes is a strong indicator for the validity of the employed model. The results of this validation method are depicted in fig. 32. The graphs in this figure clearly show that the resistivity rises as the distance between the electrodes increases and that the measurements follow a linear trend.



(a) Different top-coating thicknesses



(b) Drop-casting IL vs. IL mixed with HEMA

Figure 32: Resistance measurements validating the fitting models of fig. 30.

Additionally, the graphs in fig. 32 show that changing the thickness of the top-coating and varying the composition of IL and HEMA for drop-casting influences the resistivity whereas it did not visibly influence the degree of polymerisation when investigated with FTIR (see sec. 9.3). Since the influence of various deposition parameters on the

conductivity of the investigated samples is thoroughly discussed in the following section (sec. 10.2) it will not be further detailed here.

10.2 CONDUCTIVITY RESULTS

The conductivity of the samples was calculated after eq. 5. The length of the conductive layer, l , was measured with a sliding calliper, the thickness of the conductive layer, t , between two electrodes of the PCB via profilometry. The thickness profile was measured individually for each pair of electrodes to ensure representative results for each electrode pair for which resistivity measurements were performed. To make use of the simplifying assumptions of eq. 5 the mean value of all measured height values of the thickness profile was chosen. The resistance, R , was measured with EIS.

Tab. 6 lists the calculated conductivities of the measured samples. Conductivity values could not be calculated for all processed samples due to the following reasons: For samples obtained on substrates without pre-coating the extremely large thickness variation of the conductive layer (see fig. 23) made defining an average thickness for the calculation of the conductivity difficult. In some cases the IL did not stay on top of the PCBs during application of the top-coating via iCVD but would flow from the surface to the bottom of the substrate and remain liquid. Also ageing of the samples (see sec. 10.3) could hinder the receipt of sensible results in some cases. Multiple measurements per sample, sometimes even per electrode-pair, were performed to ensure the validity of the obtained results.

Fig. 33 shows the obtained conductivity results for samples with different parameters. Each bar represents multiple samples prepared in exactly the same way whose resistivity was measured over various electrode distances. The results show that a shorter HEMA pre-flow time increases the conductivity of the resulting film. Mixing IL with HEMA when drop-casting does not have much influence on the conductivity of the solidified IL. We can see that pre-coating the substrates leads to a decrease of conductivity, albeit still yielding good values. Also a thicker top-coating results in lower conductivity values.

The results in fig. 33 show that three sets of samples could be obtained which yield conductivity values high enough to be employed in various electrochemical applications (as proposed in the introduction of this thesis, chapter 1). Their respective conductivity values and depositions parameters are:

- $(17.6 \pm 6) \frac{\text{mS}}{\text{cm}}$ - not pre-coated, drop-casting IL only, 10 min HEMA pre-flow, 400 nm top-coating.
- $(8.3 \pm 3) \frac{\text{mS}}{\text{cm}}$ - pre-coated, drop-casting IL mixed with HEMA in a ratio 2:1, no HEMA pre-flow, 400 nm top-coating.

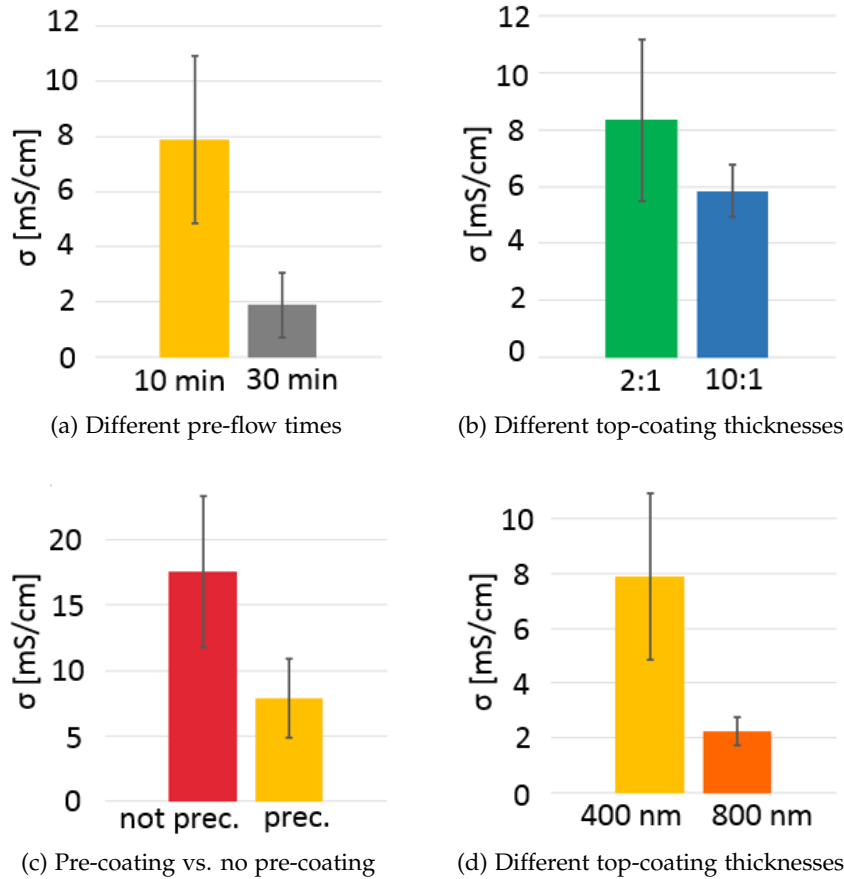


Figure 33: Effect of various deposition parameters on the resulting conductivity of the samples

- $(7.9 \pm 3) \frac{\text{mS}}{\text{cm}}$ - pre-coated, drop-casting IL only, 10 min HEMA pre-flow, 400 nm top-coating.

These results indicate that a HEMA pre-flow as low as possible, a top coating as thin as possible and drop-casting only IL or mixing it with HEMA in moderate amounts leads overall to the best conductivity values. The highest values were achieved for non-pre-coated samples but since the pre-coating greatly aids the uniformity of the obtained layers and conductivity values obtained with pre-treated samples are still high enough to employ those layers in the desired applications, it is advised to employ pre-coatings.

However, the large variations of the results in fig. 33 are still to be discussed. Those are partly due to the large thickness variations encountered in the profilometer measurements (shown in fig. 23) and to the error introduced when measuring the length of the conductive layer by hand with a sliding calliper. Additionally, the cross section of the electrodes is quite small and larger cross sections would decrease the uncertainty significantly. The majority of the introduced uncertainties could be avoided by employing electrodes

with a much larger cross-section (e.g. by performing through plane measurements), which would also require different substrates, or by producing much thinner, more even layers. Recently, a way has been shown to produce pinhole-free ion-gel films enabled by iCVD in a thickness range of tens of nano-meters [34].

Table 6: Resistivity and conductivity values of measured samples

name	d [mm]	R ₅ [ohm]	t [μm]	l [mm]	σ [mS/cm]
27.4-PCB1	1.2	4984	412	6.3	0.93
27.4-PCB2	1.2	1042	377	8.5	3.59
27.4-PCB3	1.2	543	353	9.6	6.52
27.4-PCB4	1.2	283	248	12.7	13.46
27.4-PCB5	1.2	385	121	10.0	25.76
27.4-PCB6	1.2	345	186	13.9	13.45
20.4-PCB1	1.2	981	571	9.6	2.23
20.4-PCB2	1.2	1494	298	9.1	2.96
20.4-PCB3	1.2	2032	420	10.1	1.39
25.4-PCB1	1.2	16900	98	14.7	0.49
25.4-PCB4	1.2	25080	73	14.5	0.45
25.4-PCB5	1.2	12410	9	14.7	7.31
18.5-PCB1	1.2	807	427	14.2	2.45
	0.8	630	253	14.2	3.53
18.5-PCB2	1.2	2312	319	14.2	1.15
18.5-PCB4	1.2	720	225	13.9	5.33
	0.8	471	156	13.9	7.83
18.5-PCB5	1.2	924	258	13.2	3.81
18.5-PCB6	1.2	682	183	13.2	7.28
3.7-PCB1	1.6	1700	118	12.1	6.59
	1.6	2200	118	12.1	5.09
	1.6	1800	118	12.1	6.23
	1.2	1000	90	12.9	10.34
	1.2	1200	90	12.9	8.61
	1.2	640	90	12.9	16.15

Table 6: Continued: Resistivity and conductivity values of measured samples

name	d [mm]	R ₅ [ohm]	t [μm]	l [mm]	σ [mS/cm]
3.7-PCB2	0.8	556	101	13.3	10.71
	0.8	744	101	13.3	8.00
	0.8	538	101	13.3	11.07
	1.6	1700	119	12.8	6.18
	1.6	2400	119	12.8	4.38
	1.2	795	118	13.8	9.27
	1.2	1300	118	13.8	5.67
	1.2	812	118	13.8	9.08
3.7-PCB5	0.8	1100	124	13.6	4.31
	0.8	1100	124	13.6	4.31
	0.8	600	124	13.6	7.91
	1.6	2800	179	13.4	2.38
	1.6	2800	179	13.4	2.38
	1.2	2400	180	14.3	1.94
	1.2	2600	180	14.3	1.79
	1.2	2700	180	14.3	1.73
3.7-PCB6	0.8	1900	189	12.9	1.73
	0.8	1900	189	12.9	1.73
	0.8	1600	189	12.9	2.05
	1.6	3100	188	10.2	2.69
	1.6	3000	188	10.2	2.78
	1.2	1500	175	13.3	3.44
10.7-PCB1	1.2	2000	175	13.3	2.58
	1.6	2000	113	8.9	7.95
	1.2	891	130	9.4	11.02
	1.2	909	130	9.4	10.80
10.7-PCB2	0.8	983	135	8.9	6.77
	1.6	3100	103	8.9	5.63
	1.6	3100	103	8.9	5.63
	1.6	3300	103	8.9	5.29
10.7-PCB3	1.2	1100	87	8.6	14.58
	0.8	1200	109	8.6	7.11
	0.8	1000	109	8.6	8.53
	1.6	3000	114	8.5	5.50
	1.2	1200	167	11.6	5.16

Table 6: Continued: Resistivity and conductivity values of measured samples

name	d [mm]	R ₅ [ohm]	t [μm]	l [mm]	σ [mS/cm]
10.7-PCB ₄	1.2	1100	167	11.6	5.63
	0.8	845	151	12.1	5.18
	0.8	859	151	12.1	5.10
	1.6	7300	87	3.6	7.00
	1.2	3400	83	5.5	7.73
10.7-PCB ₅	0.8	1800	119	6.8	5.49
	1.6	4800	129	10.6	2.44
	1.2	3300	188	11.5	1.68
	0.8	2800	137	11.3	1.85
	0.8	2700	137	11.3	1.91
10.7-PCB ₆	0.8	2700	137	11.3	1.91
	1.6	4400	110	8.9	3.71
	1.6	3800	110	8.9	4.30
	1.2	2600	121	8.6	4.44
	0.8	1800	146	8.6	3.54

10.2.1 Comparison to Literature Values

A comparison of the results obtained from the conducted experiments to literature values shows, that up to more than 1/2 of the original conductivity of the liquid IL can be contained in the solidified layer. Comparisons were made with a value noted by the chemical supplier Sigma Aldrich [35] for 1-ethyl-3-methylimidazolium dicyanamide (EMID) ($27 \frac{\text{mS}}{\text{cm}}$), an IL very similar to the used AMID, only differing in one CH_x bond. The counter ion, which is responsible for the ionic conductivity of the IL is the same for both ILs making it save to assume a similar conductivity value for AMID than for EMID. The structure of EMID is shown in fig. 34.

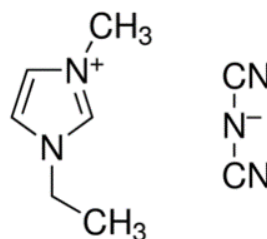
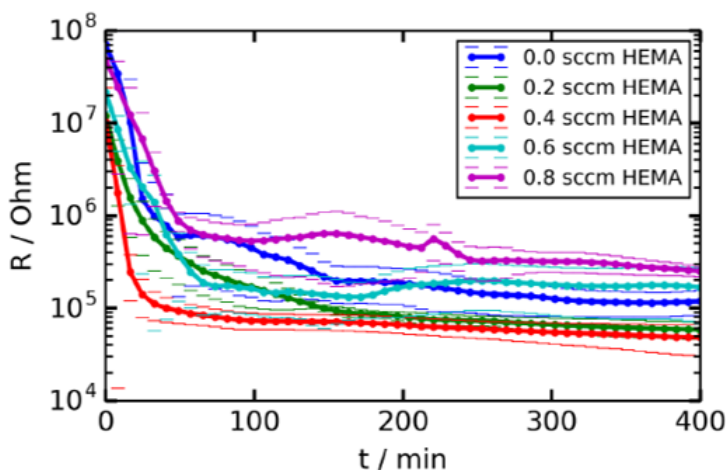


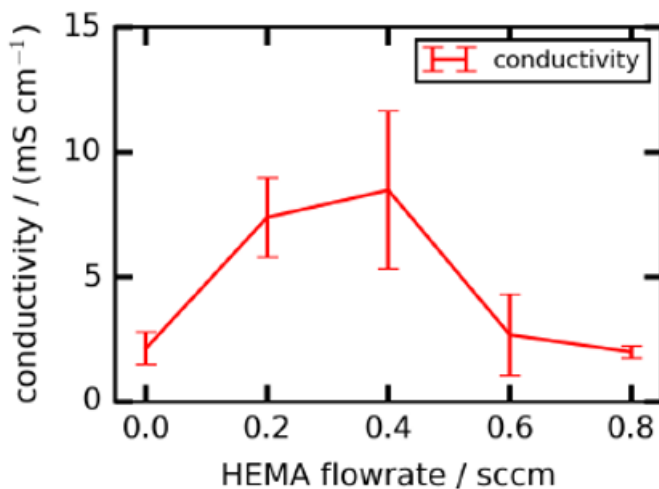
Figure 34: Chemical structure of 1-ethyl-3-methylimidazolium dicyanamide

10.2.2 Comparison to Previous Studies

When comparing the obtained conductivity results to previously studies of ion conductive ionomers consisting of methacrylic acid (MAA), HEMA and EGDMA the experiments conducted for this thesis yield similar results. Fig. 35, which contains results from the master's thesis of M. Tazreiter [22], shows that the highest obtained conductivity values for previously measured ionomers lie at $(8 \pm 3) \frac{\text{mS}}{\text{cm}}$.



(a) Equilibration time for EIS measurements



(b) Achieved conductivity values

Figure 35: Conductivity of p-MAA-HEMA-EGDMA. Resistivity measurements performed by EIS in humidity levels $\geq 95\%$. - Measurements performed by M. Tazreiter, figure reprinted from [22].

Although the studies conducted in [22] yielded partly similar results, it is important to note that the measurements presented in fig. 35 were performed in very high humidity ($\geq 95\%$) whereas the

results in fig. 33 were obtained by resistivity measurements in ambient air. Furthermore, the ionomer films took long times to equilibrate to the high humidity until the value was stable enough to be measured as visible in fig. 35a. In contrast, the ambient air measurements of the solidified ILs were stabilised and ready for measurement after a few seconds, since no equilibration process with its surroundings was necessary.

10.3 AGEING OF SAMPLES

To investigate the ageing behaviour of the samples, two samples on PCBs were prepared exactly in the same way. One had its resistance measured with EIS multiple times over the course of a month, the other was placed in a glove box to keep it from atmosphere. The results are depicted in fig. 36. The resistivity results show that the sample kept in atmosphere aged rapidly whereas the sample that was kept in the glove-box only showed a small rise in resistivity.

Each sample was measured over three different electrode pairs to ensure that the measurements made sense. Since the only difference between the two samples was, that the one was kept in a non-humid environment, the ageing can likely be attributed to water uptake of the polymer and IL on the surface of the substrate. Since the electrodes on the PCBs consist mainly of copper covered by a thin layer of gold, also corrosion is a possible explanation for the rapid ageing of the sample.

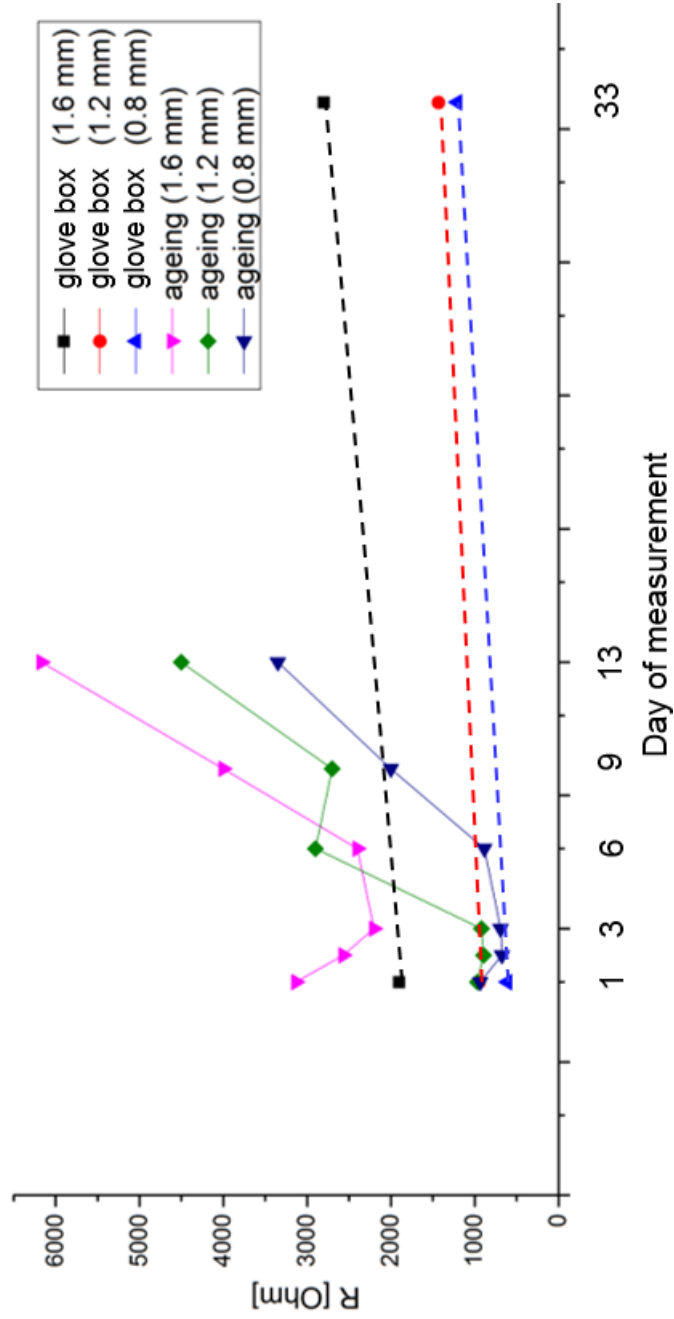


Figure 36: Measured resistance of an ageing sample vs. a non-ageing sample.

CONCLUSION AND OUTLOOK

By coating droplets of liquid IL with a p(HEMA-EGDMA) layer via iCVD, solidified IL membranes were obtained which showed promising conductivity values in ambient air.

Profilometry and dCAM measurements proved that pre-coating the substrates before depositing liquid IL by drop-casting onto them resulted in better spreading of the IL and also lead to more uniform solid films. FTIR measurements also showed that pre-coating the substrates aids the polymerisation of the IL.

Many other tuned deposition parameters such as using different amounts of IL, changing the HEMA pre-flow time, choosing a different thickness for the top-coating vs. drop-casting IL or IL mixed with liquid HEMA yielded no visible changes for the degree of polymerisation. FTIR measurements also clearly showed that the IL was only partly polymerised as some of peaks representing the vinyl bonds remained.

When determining the conductivity of the produced samples from the resistivity values measured with EIS, values as high as $(17.6 \pm 6) \frac{\text{mS}}{\text{cm}}$ could be obtained by measurements in ambient air. This means that more than 1/2 of the original conductivity of the liquid IL can be contained. Although previous studies yielded comparative results, the studied ionomers ionomers (pMAA-HEMA-EGDMA), which yielded a maximum conductivity value of $(8 \pm 3) \frac{\text{mS}}{\text{cm}}$, had to be measured in very high humidity ($\geq 95\%$).

Additionally, it was shown that HEMA pre-flow time, pre-coating the substrate and thickness of the top-coating influence the conductivity of the sample. The best conductivity values were achieved for drop-casting pure IL, employing a HEMA pre-flow as short as possible while still solidifying the IL (10 min) and using a top-coating as thin as possible (400 nm). Although the best conductivity values were obtained for non-pre-coated samples also pre-coated samples showed favourable results comparable to previous studies while greatly increasing the uniformity of the layer.

However, the conductivity results show large uncertainties due to large thickness variations of the solidified IL and the small cross section of the electrodes. For the future it is advised to either change to through plane measurements, which means that either different substrates would have to be used, bringing new challenges with them, or much thinner layers would have to be produced.

BIBLIOGRAPHY

- [1] et al. A.M. Pappa. "Polyelectrolyte layer-by-layer assembly on organic electrochemical transistors." In: *ACS Appl. Mater. Interfaces* 9.12 (2017), pp. 10427–10434.
- [2] et al. H. Ye. "New membranes based on ionic liquids for PEM fuel cells at elevated temperatures." In: *Journal of Power Sources* 178 (2008), pp. 651–660.
- [3] et al. Yun Wang. "A review of polymer electrolyte membrane fuel cells: Technology, applications, and needs on fundamental research." In: *Applied Energy* 88 (2011), pp. 981–1007.
- [4] ed. by K.K. Gleason. *CVD Polymers – Fabrication of Organic Surfaces and Devices*. 2015.
- [5] University of York. *The Essential Chemical Industry Online - Polymers: An Overview*.
- [6] Y. Zhang X. Liu A. Zhang G. Su T. Zhou. "Microdynamics Mechanism of D₂O Absorption of the Poly(2-hydroxyethyl methacrylate)-based Contact Lens Hydrogel Studied by Two-dimensional Correlation ATR-FTIR Spectroscopy." In: *Soft Matter* 12.4 (2016), 1145 – 1157.
- [7] Wei-Fang Su. *Principles of Polymer Design and Synthesis*. Springer, 2013.
- [8] George Odian. *Principles of Polymerization*. John Wiley and Sons, 1970.
- [9] R.F.T. Stepto U.W. Suter A.D. Jenkins P. Kratochvíl. "Glossary of Basic Terms in Polymer Science." In: *Pure and Applied Chemistry* 68 (1996), pp. 2287–2311.
- [10] J.S. Cooper V. Mehta. "Review and Analysis of PEM Fuel Cell Design and Manufacturing." In: *Journal of Power Sources* 114 (2003), pp. 32–53.
- [11] K. Lian H. Gao. "Proton-conducting polymer electrolytes and their applications in solid supercapacitors: a review." In: *RSC Advances* 62 (2014), 33091–33113.
- [12] H. Zhang J. Zhang J. Zhang J. Wu. *PEM Fuel Cell Testing and Diagnosis*. Elsevier, 2013.
- [13] Institute of Organic Chemistry Johannes Gutenberg University of Mainz. *The Essential Chemical Industry Online - Polymers: An Overview*.
- [14] Madhulata Shukla and Satyen Saha. *Ionic Liquids – New Aspects for the Future*. 2013.

- [15] K.K. Gleason K.K.S. Lau. "Initiated Chemical Vapor Deposition (iCVD) of Poly(alkyl acrylates): An Experimental Study." In: *Macromolecules* 39 (2006), pp. 3688–3694.
- [16] et al. A.M. Coclite. "25th Anniversary Article: CVD Polymers: A New Paradigm for Surface Modification and Device Fabrication." In: *Advanced Materials* 25 (2013), 5392 – 5423.
- [17] K.K. Gleason K.K.S. Lau. "Initiated Chemical Vapor Deposition (iCVD) of Poly(alkyl acrylates): A Kinetic Model." In: *Macromolecules* 39 (2006), 3695 – 3703.
- [18] K.K. Gleason W.E. Tenhaeff. "Initiated and Oxidative Chemical Vapor Deposition of Polymeric Thin Films: iCVD and oCVD." In: *Advanced Functional Materials* 18 (2008), pp. 979 –992.
- [19] M. Gupta L.C. Bradley. "Encapsulation of Ionic Liquids within Polymer Shells via Vapor Phase Deposition." In: *Langmuir* 28.27 ().
- [20] Gamry Instruments. *Basics of Electrochemical Impedance Spectroscopy*.
- [21] S. Kjelstrup J. M. Rubi. "Mesoscopic Nonequilibrium Thermodynamics Gives the Same Thermodynamic Basis to Butler-Volmer and Nernst Equations." In: *The Journal of Physical Chemistry* 107.48 (2003), 13471–13477.
- [22] Martin Tazreiter. "Proton conductivity measurements on standard and custom ionomers." Master's Thesis. Graz University of Technology, 2017.
- [23] Y.M. Lee R.D. Lee C.H. Lee H.B. Park. "Importance of Proton Conductivity Measurement in Polymer Electrolyte membrane for Fuel Cell Application." In: *Ind. Eng. Chem. Res.* 44 ().
- [24] B. Rodger D. Loveday P. Peterson. *Evaluation of Organic Coatings with Electrochemical Impedance Spectroscopy - Part 2: Application of EIS to Coatings*.
- [25] J. R. Macdonald ed. by E. Barsoukov. *Impedance Spectroscopy: Theory, Experiment, and Applications*. John Wiley and Sons, 2005.
- [26] Gamry Instruments. *EIS: Potentiostatic or Galvanostatic Mode?*
- [27] Paul Christian. "Polymer Thin Films by initiated Chemical Vapor Deposition - From Proton Conduction to the Encapsulation of Pharmaceuticals." PhD Thesis. Graz University of Technology, 2018.
- [28] J.A. Woolam Co. *Ellipsometry Tutorial*.
- [29] J.A. Woolam Co. *CompleteEASE Data Analysis Manual*.
- [30] attention. *Theory Note 1 - Static and dynamic contact angles and their measurement techniques*.
- [31] Nano Science Instruments. *How a Profilometer Works*.

- [32] Bing Yan Hans-Ulrich Gremlich. *Infrared and Raman Spectroscopy of Biological Materials*. Marcel Dekker Inc, 2000.
- [33] M. Tazreiter et al. "Simple method for the quantitative analysis of thin copolymer films on substrates by infrared spectroscopy using direct calibration." In: *Analytical Methods* 9 (2017), pp. 5266–5273.
- [34] Andong Liu. "Mechanically Flexible Vapor-Deposited Polymeric Thin Films for Electrochemical Devices." PhD Thesis. Massachusetts Institute of Technology, 2017.
- [35] Sigma Aldrich. *Ionic Liquids for Electrochemical Applications*.